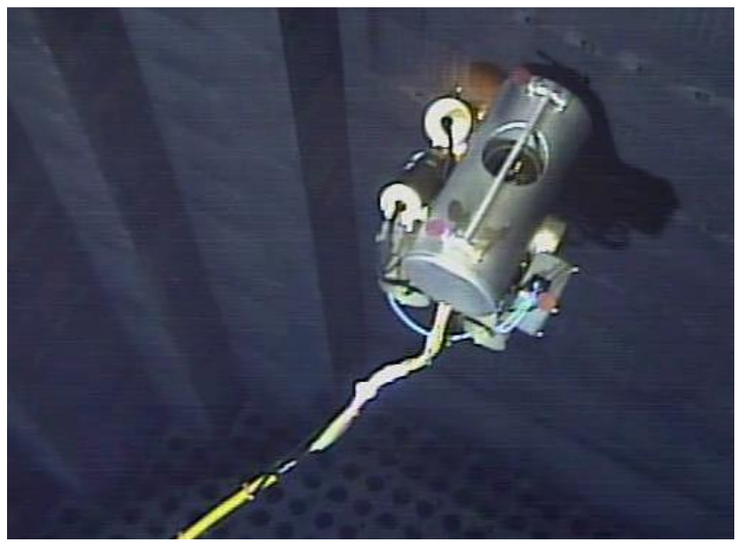

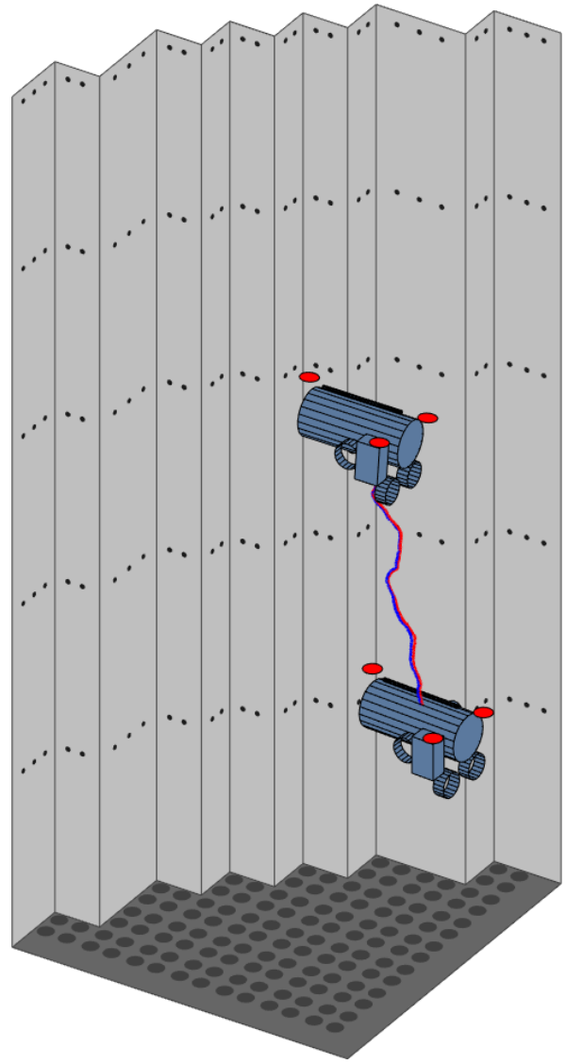

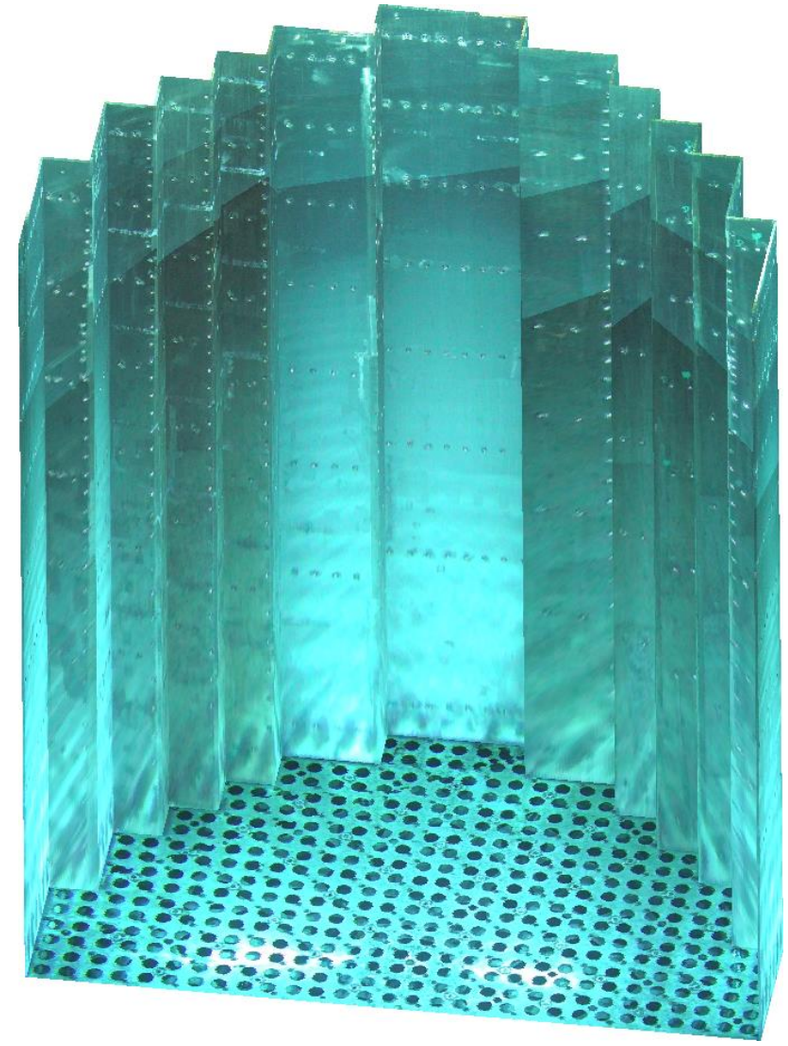

State Estimation and Localization for ROV-Based Reactor Pressure Vessel Inspection Using a Pan-Tilt-Zoom Camera

Timothy E. Lee
Carnegie Mellon University

M.S. in Robotics Speaking Qualifier
Friday, August 4, 2017

Carnegie Mellon University
The Robotics Institute

Outline

Introduction

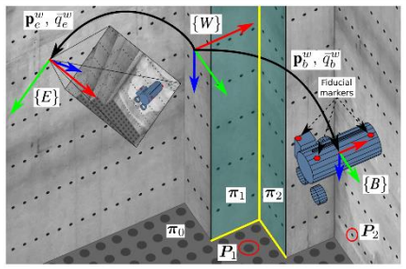

System Models and Methods

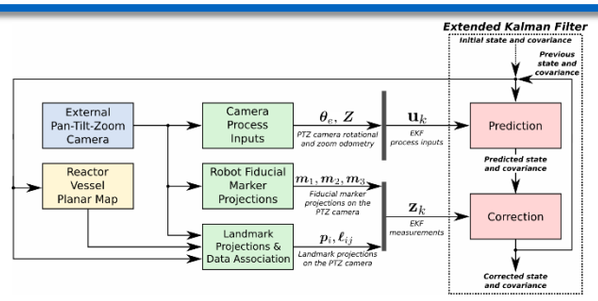

State Estimation and Localization

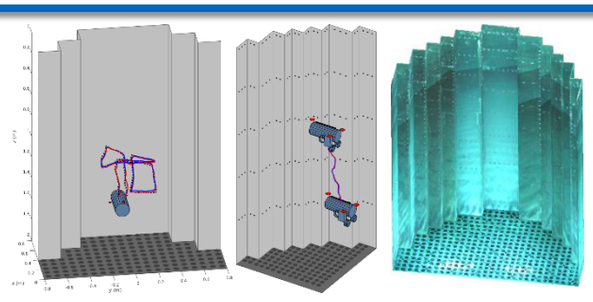

Results

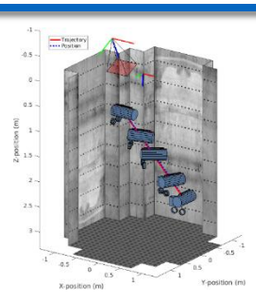

Conclusion and Future Work

Outline

Introduction

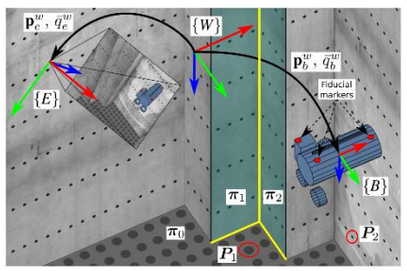

System Models and Methods

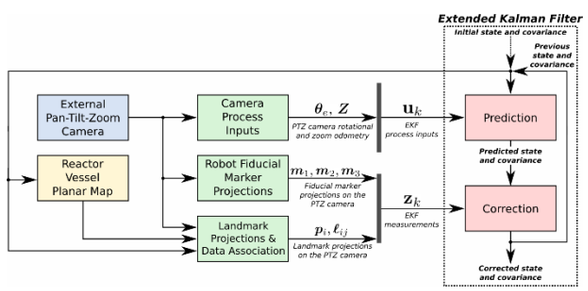

State Estimation and Localization

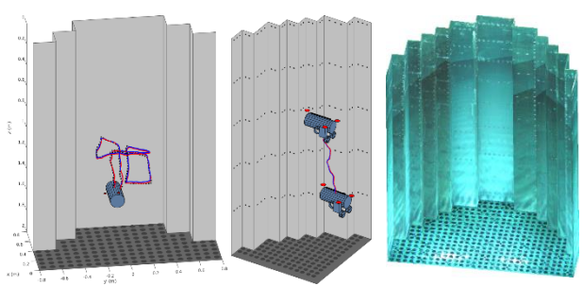

Results

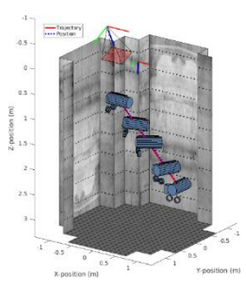

Conclusion and Future Work

Background and Problem Statement

- The reactor pressure vessel of a nuclear power plant must be inspected periodically to assess its structural integrity.
  - Embrittlement, stress cracking, and flow induced vibration are some mechanisms that impact reactor integrity.
- Vessel inspections are typically scheduled during refueling outages. Recently, outages last six weeks on average.[1]
- Existing human-in-the-loop inspection techniques are costly, leading to an interest in robotics technologies.
- Improving inspection efficiency via automation will yield shorter outages and decreased radiation dosage to personnel.

[1]U.S. Energy Information Administration.

Reactor Pressure Vessels

[1]U.S. Nuclear Regulatory Commission.

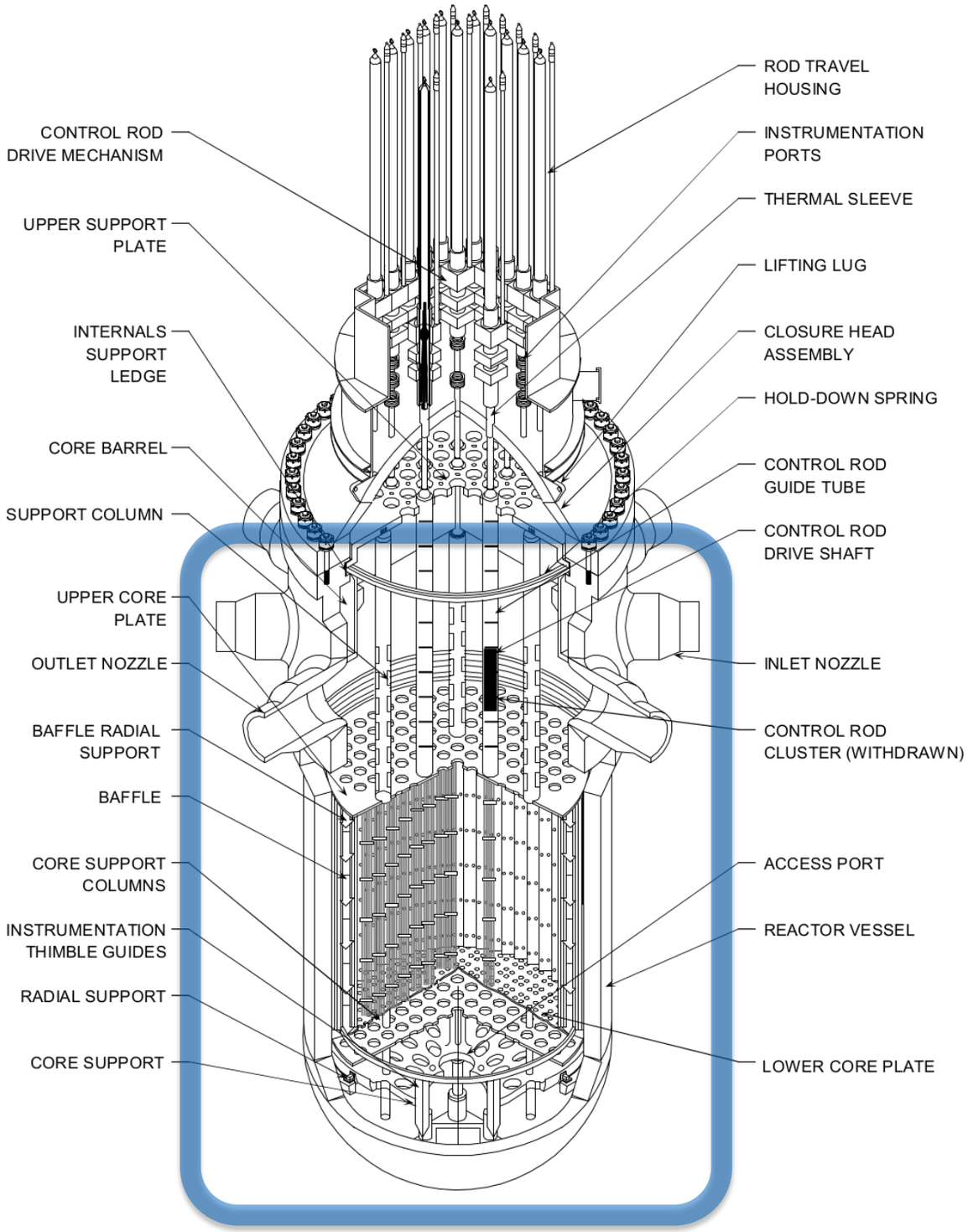

Diagram of a Pressurized Water Reactor (PWR)[1]

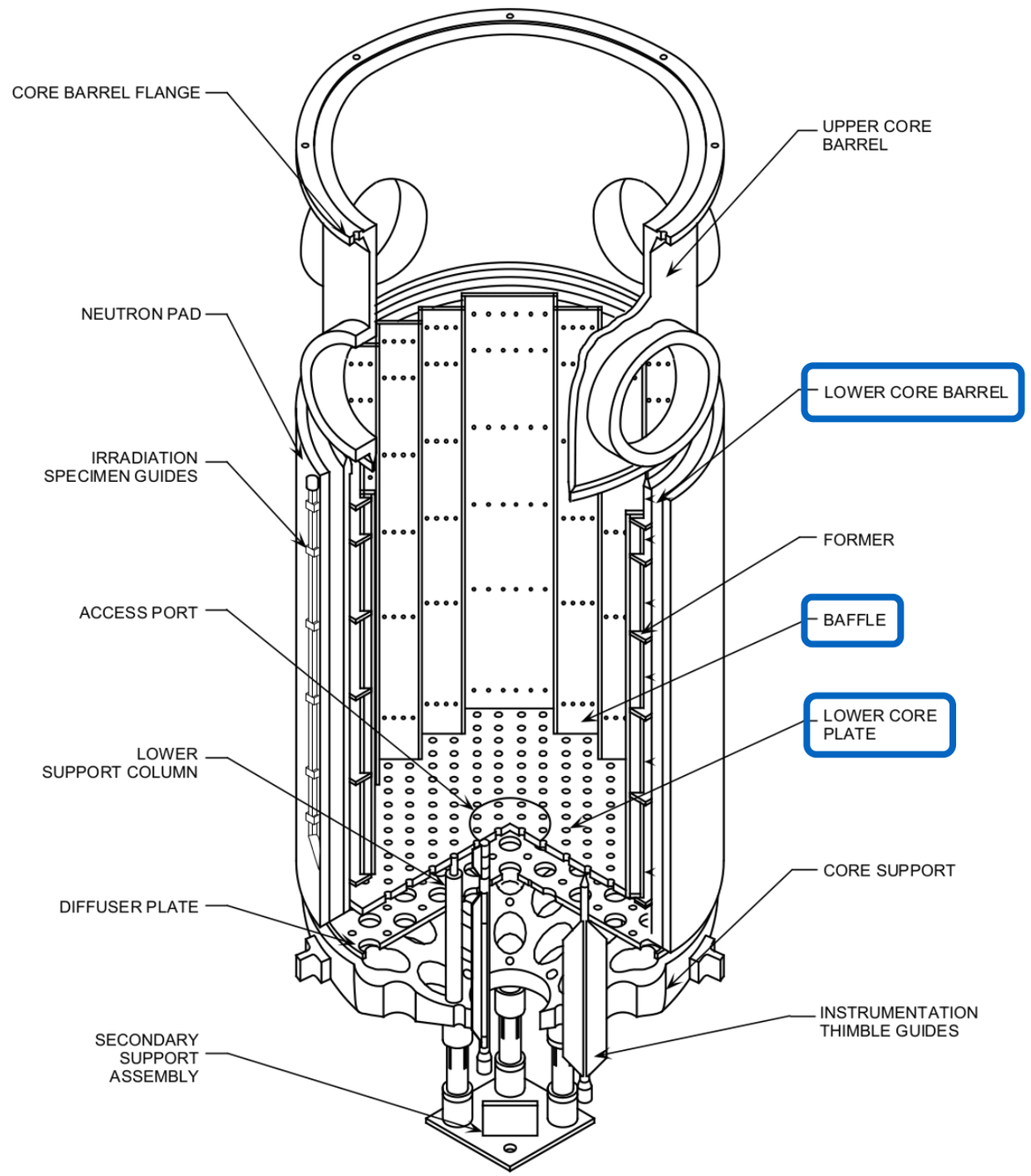

Diagram of the Lower Internals of a PWR[1]

ROV-Based RPV Inspection

We seek to automate the inspection of nuclear reactor pressure vessels via a remotely operated vehicle (ROV).

Video of an ROV inspecting a nuclear reactor core.

Environmental Constraints for ROV Sensing

- Baffle plates emits radiation up to 30 kRad/hr
  - Destroys non-hardened electronics
  - Sufficiently hardened sensors are extremely noisy, prohibitively expensive, and difficult to integrate with platform
- Radiation field weakens rapidly in water
  - A reduction of an order of magnitude every 16 inches
- The water in a nuclear reactor is free of turbidity

External Camera

Thesis Problem: ROV Localization

- A **pan-tilt-zoom (PTZ) camera** meets the unique sensing constraints of the environment.

- We are motivated to develop a methodology that enables **ROV localization** within the reactor lower core using a PTZ camera.

- For use in reactor inspections, we also address:
  - Online initialization for system efficiency and utility
  - Robustness to a known radiation failure mode (speckling)

Research Challenges

- Environmental and platform constraints on sensing
- Limited to methodologies that can easily be integrated into existing reactor inspection processes
- Field experiments are challenging
- Required advances in both robotics science and systems
  - Development of a sensing solution for the environment
  - Development of algorithms that work in practice

Contributions of this Work

1. A **framework that enables ROV localization within the reactor lower core** using a PTZ camera that provides pose estimates in three dimensions, *including the systems that enable this framework*.
2. A **planar representation of the reactor core geometry** as a map for localization.
3. Demonstrations of **framework accuracy and robustness** to speckling.
4. Methodology for **online initialization** for use during reactor inspections.

Outline

Introduction

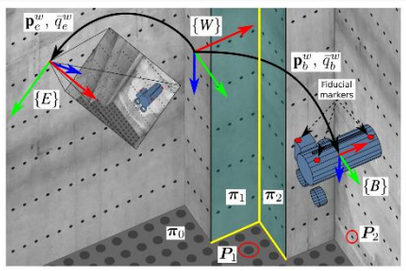

System Models and Methods

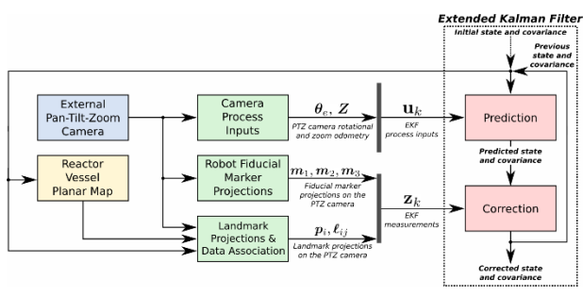

State Estimation and Localization

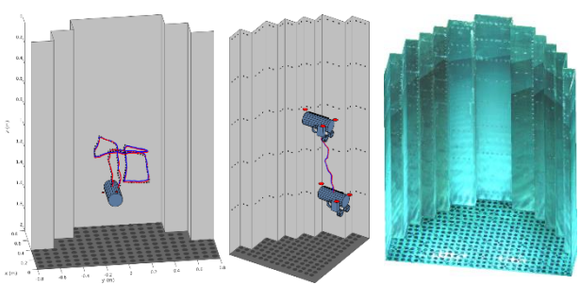

Results

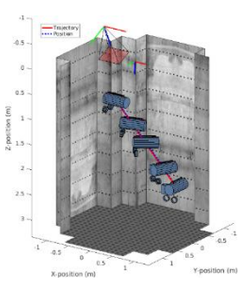

Conclusion and Future Work

System Overview

- The system can be represented using several frames:
  - **ROV body frame** *{B}*, located at robot center of mass
  - External, **pan-tilt-zoom camera frame** *{E}*
  - **World frame** *{W}*, in which the reactor geometry is defined

System Representation and Landmarks

- 6DOF poses represented by position and quaternion
- Projection of 3D points yield 2D points in the image
- Projection of 3D lines yield 2D lines in the image
- 3D lines arise from the intersection of vessel surfaces

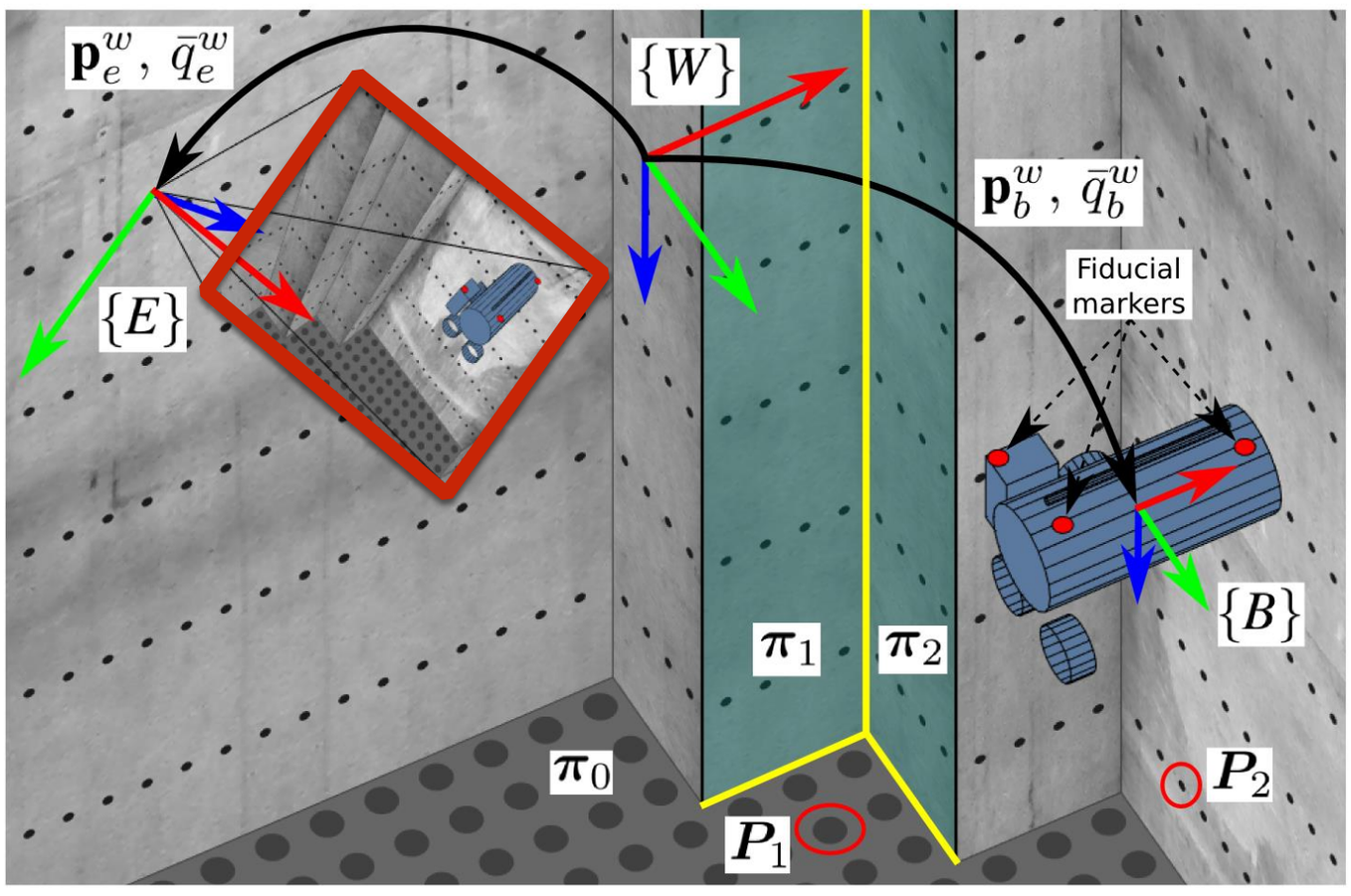

Three-dimensional system representation.

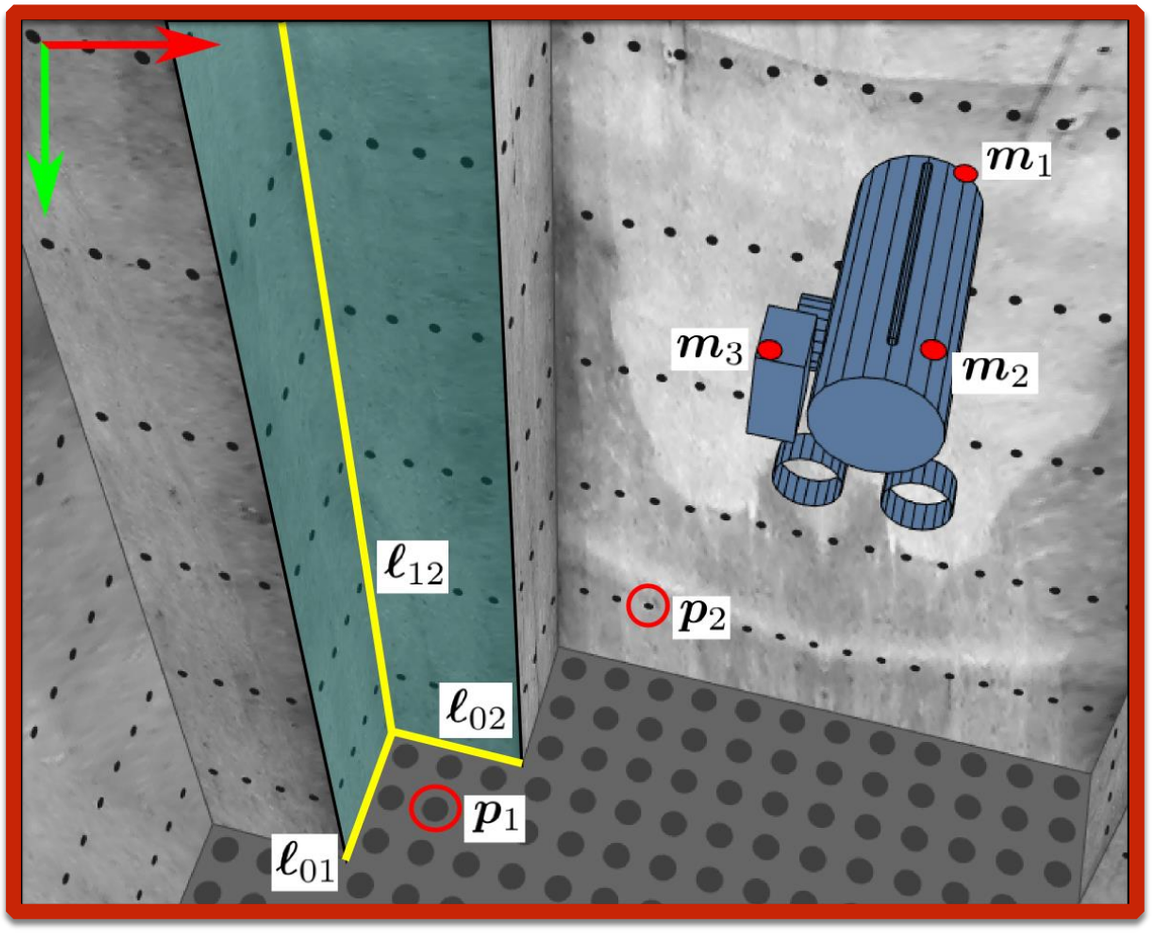

Two-dimensional system representation.

PTZ Camera Models: Point Projection

- Camera represented as a pinhole projection model
  - Mapping from $\mathbb{P}^3 \mapsto \mathbb{P}^2$
  - Homogeneous coordinates:
    - 3D point: $\widetilde{\boldsymbol{P}} \sim [\boldsymbol{P}^{\mathrm{T}}, 1]^{\mathrm{T}}$
    - 2D point: $\widetilde{\boldsymbol{p}} \sim [\boldsymbol{p}^{\mathrm{T}}, 1]^{\mathrm{T}}$

$$\widetilde{\boldsymbol{p}} \sim K[\,R\,|\,\mathbf{t}\,]\widetilde{\boldsymbol{P}}$$

$$K = \begin{bmatrix} f_x & 0 & c_x \\ 0 & f_y & c_y \\ 0 & 0 & 1 \end{bmatrix}$$

- Focal length components vary with zoom
- Assume a fixed principal point that is congruent with the center of zoom[1]

[1]Wu and Radke (2013).

PTZ Camera Models: Line Projection

- This camera model causes the following line projection:
  - Mapping from $\mathbb{P}^5 \mapsto \mathbb{P}^2$
  - 3D (Plücker) line: $\boldsymbol{\mathcal{L}} \in \mathbb{P}^5$
  - 2D line: $\boldsymbol{\ell} \in \mathbb{P}^2$

$$\boldsymbol{\ell} \sim \mathcal{K}\mathcal{D}\boldsymbol{\mathcal{L}}$$

$$\mathcal{K} = \begin{bmatrix} \det(K)\, K^{-\mathrm{T}} & 0_{3\times 3} \end{bmatrix}$$

- Line projection matrix
- Rigid displacement matrix
- Analogous to K and [R | t] for points

$$\mathcal{D} = \begin{bmatrix} R & [\mathbf{t}]_\times R \\ 0_{3\times 3} & R \end{bmatrix}$$

[1]Bartoli and Sturm (2004).

PTZ Camera Models: Orientation

- PTZ camera has two degrees of freedom: pan and tilt with respect to a base “scene frame”
  - Pan axis fixed w.r.t. scene frame
  - Tilt axis fixed w.r.t. camera frame
- Camera orientation w.r.t world frame obtained from kinematic chain:[1]

$$R_e^w = R(R_s, \theta, \phi) = R_\phi R_\theta R_s$$

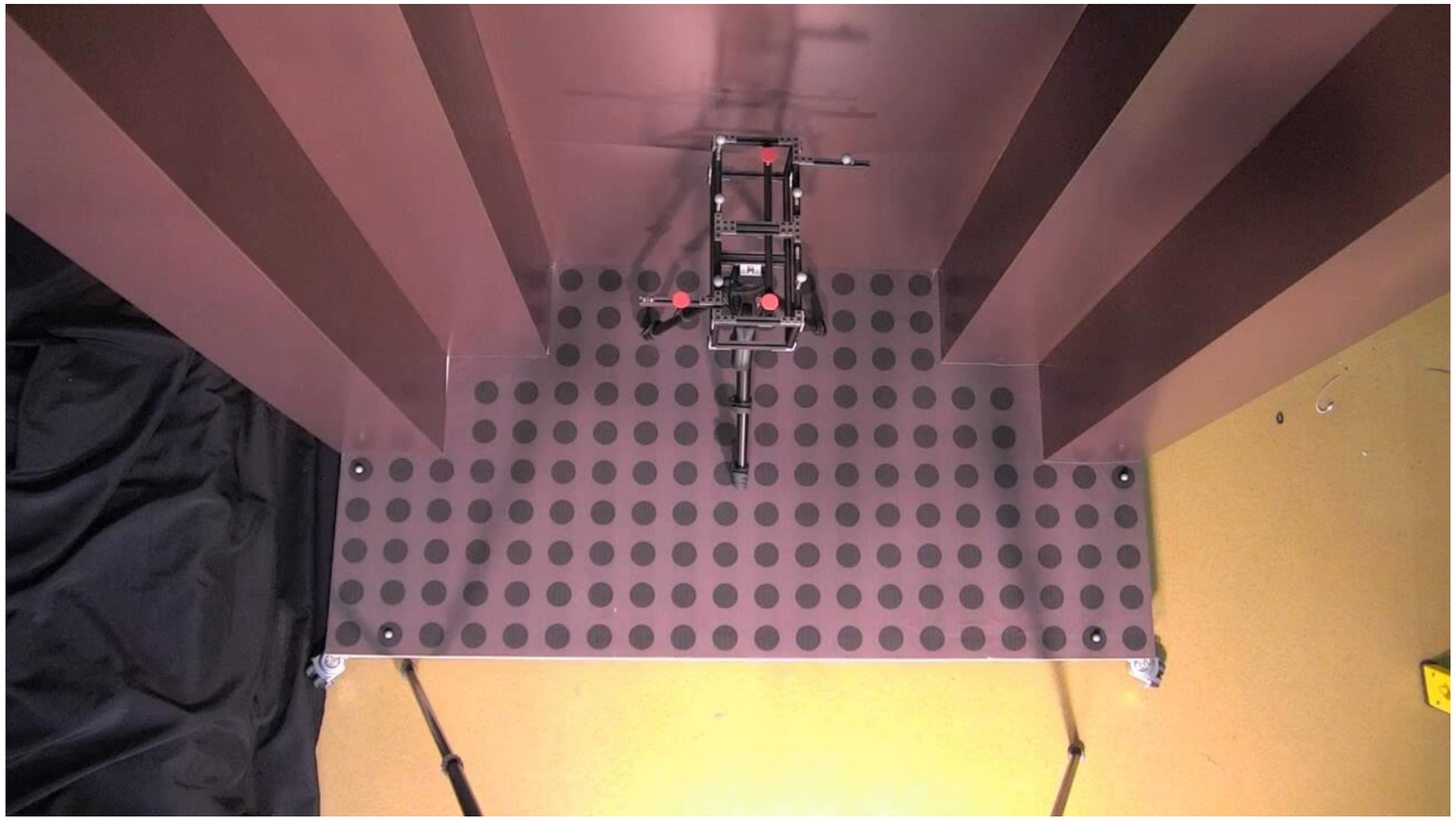

[1]Collins and Tsin (1999).

Underwater Optics

- In an underwater setting, **the camera optics are inherently coupled with the type of camera housing**
- In water with an ideal spherical housing, there is no change to the image field of view under some conditions
- Estimate both focal length components to account for underwater optics with partially known optical model

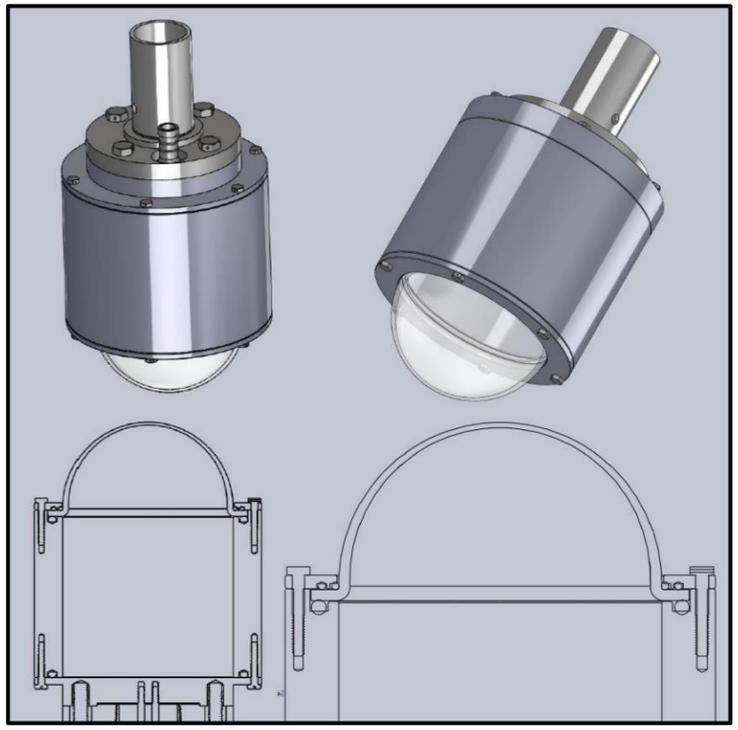

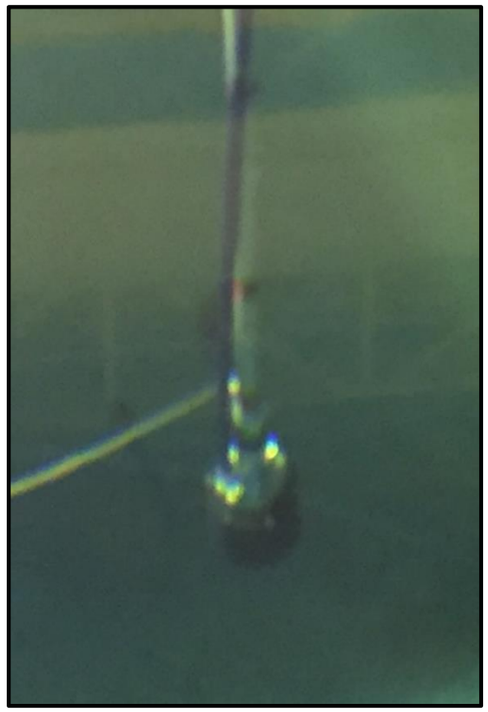

ROV and Fiducial Markers

- ROV pose is estimated from projections of fiducial markers mounted on the platform
- Assume that the position of the markers in the body frame is known to a limited uncertainty

$$\widetilde{\boldsymbol{m}}_i \sim K\,[\,R_w^e \,|\, \mathbf{t}_w^e\,]\,T_b^w\,\widetilde{\boldsymbol{M}}_i^b$$

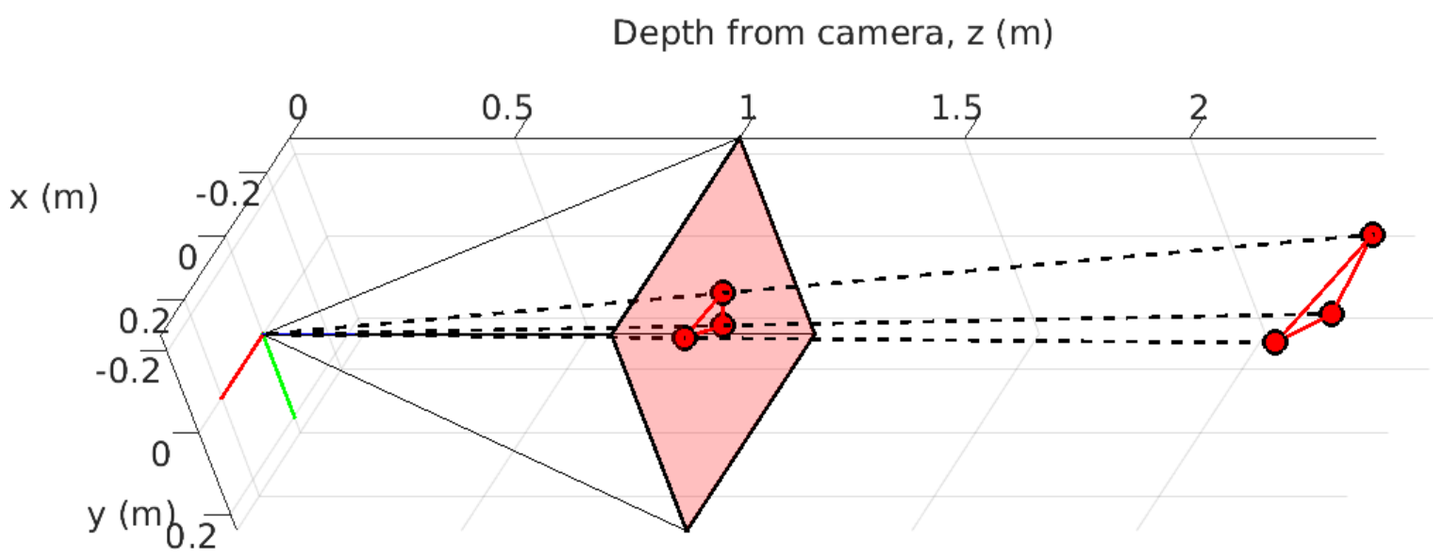

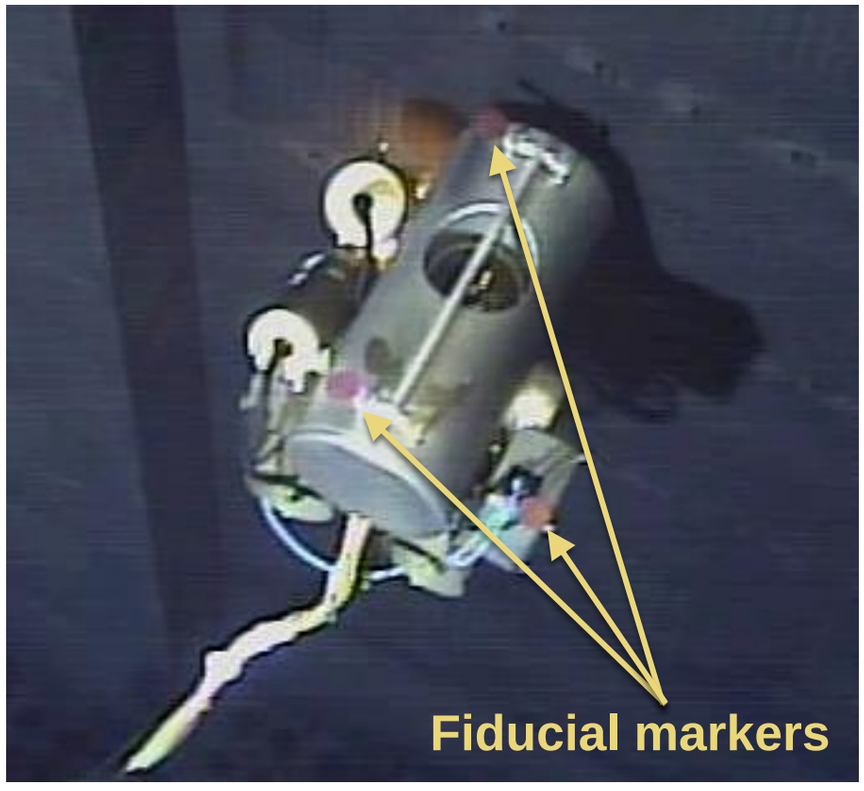

Vessel Geometry

- The lower core consists of the following components:
  - Core plate, forming the reactor "floor"
  - Baffle plates, forming the reactor "walls"

- Landmarks only on planar surfaces
- Lines arising at the intersection of planar surfaces

- Fuel assemblies are removed during inspection

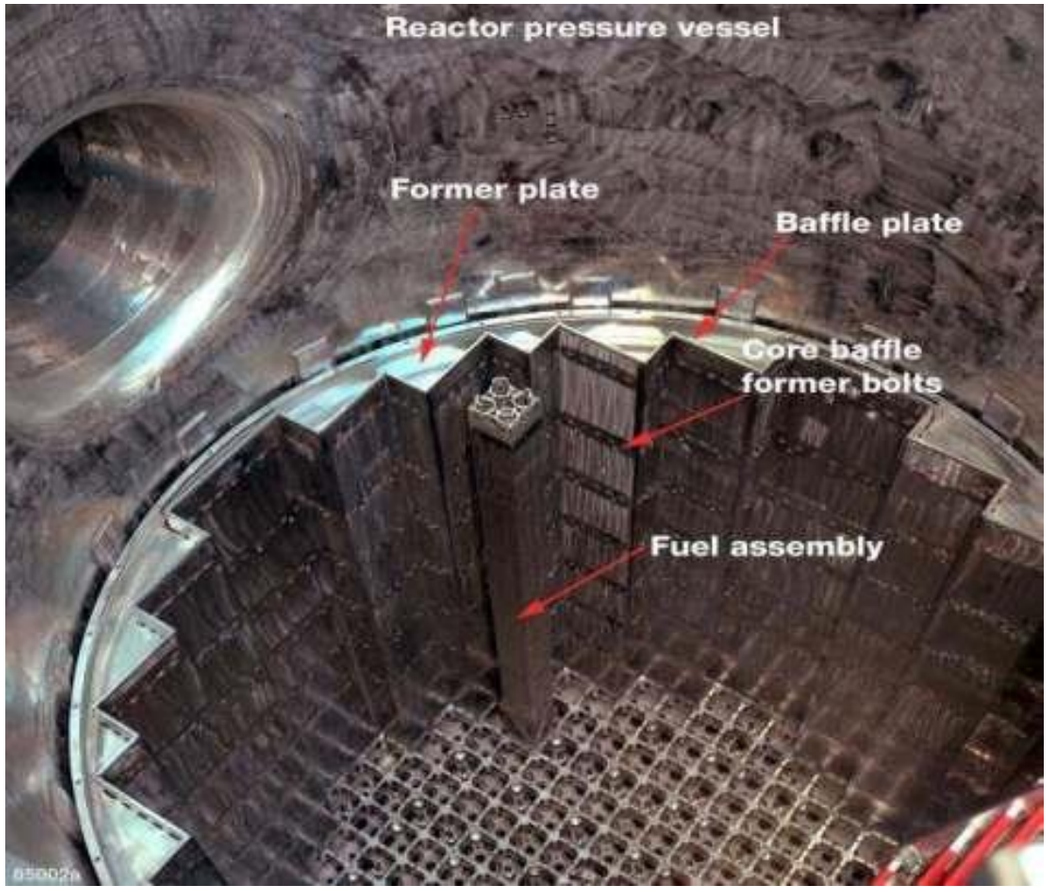

Diagram of the reactor lower core.[1]

[1]Westinghouse Electric Company, LLC.

Vessel Geometry: Representative Examples

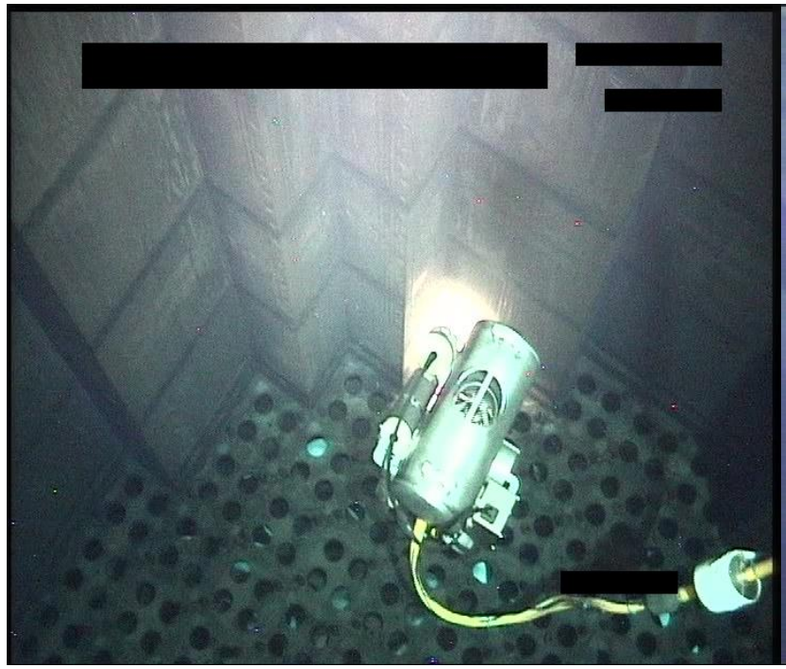

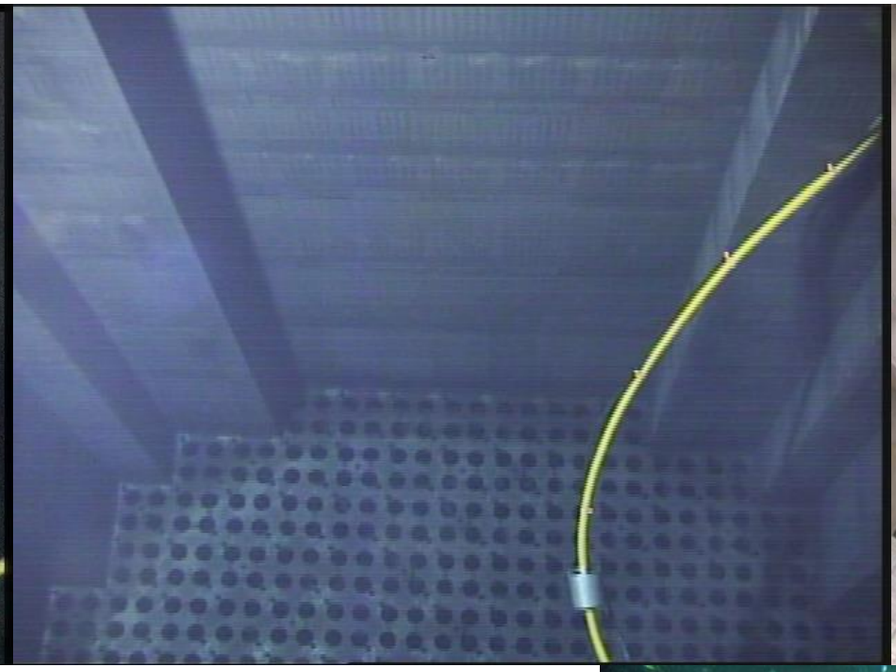

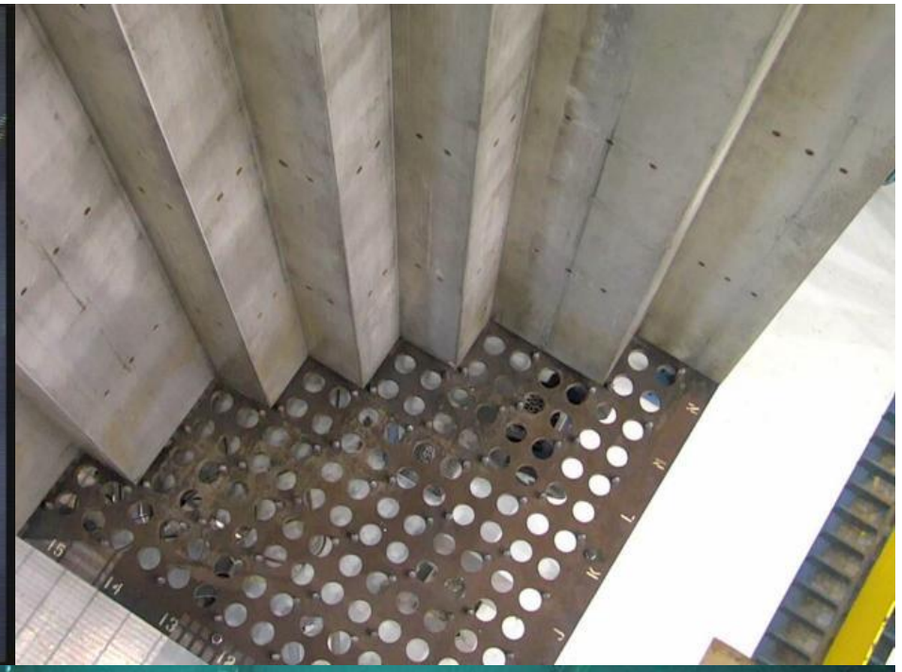

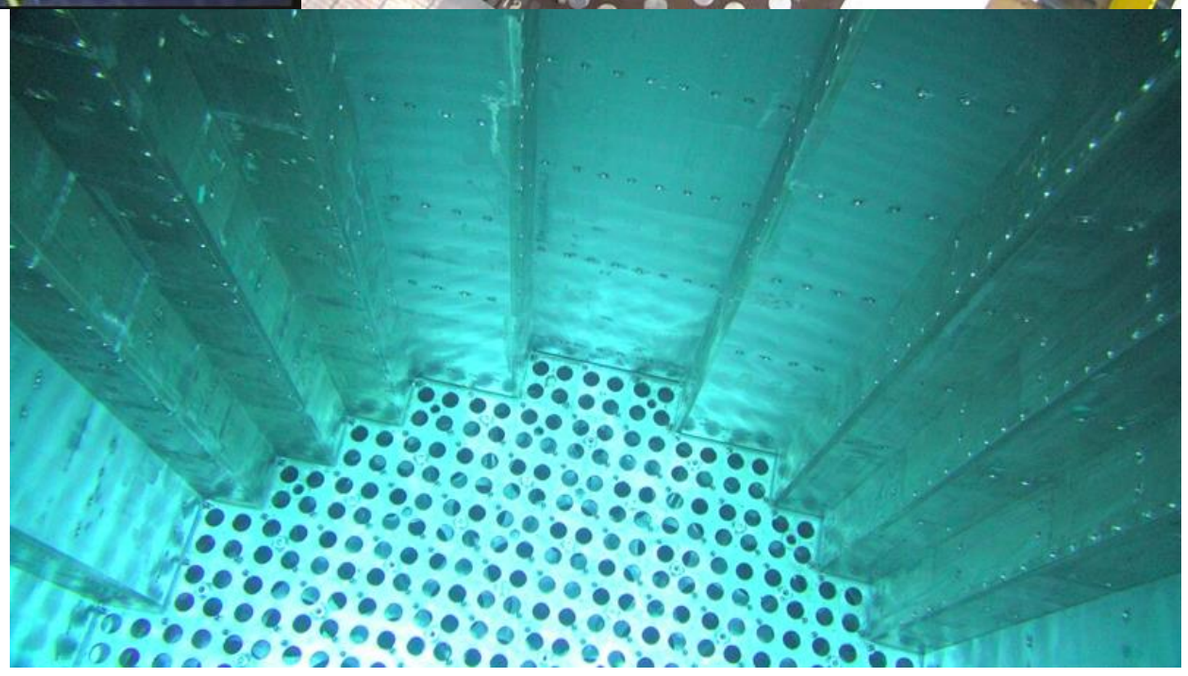

- Minor structural variation
  - Vessel size
  - Quantity of baffle plates
- Visual differences
  - Core plate flow holes are typically apparent
  - Landmarks on baffle plates may not always be visible

Vessel Geometry: Planar Representation

- Represent the reactor geometry as a series of planes, and points that are coplanar on these planes.
- Reactor surfaces as planes: $\boldsymbol{\pi} = [\,\bar{n}^{\mathrm{T}},\, d\,]^{\mathrm{T}} \in \mathbb{R}^4$
- Point coplanarity constraint: $\boldsymbol{\pi} \cdot \widetilde{\boldsymbol{P}} \;=\; 0$
- Projections of points and lines provide landmarks used for localization:

$$\widetilde{\boldsymbol{p}}_i \sim K\,[\,R_w^e \,|\, \mathbf{t}_w^e\,]\,\widetilde{\boldsymbol{P}}_i^w$$

$$\mathcal{L}_{ij} = \boldsymbol{\pi}_i \wedge \boldsymbol{\pi}_j$$

$$\boldsymbol{\mathcal{L}}_{ij}^w \sim \begin{bmatrix} d_i\bar{n}_j - d_j\bar{n}_i \\ \\ \bar{n}_i \times \bar{n}_j \end{bmatrix}$$

$$\boldsymbol{\ell}_{ij} \sim \mathcal{K}\mathcal{D}_w^e \boldsymbol{\mathcal{L}}_{ij}^w$$

Speckling

- Speckling is stochastic chromatic image noise that is induced by radiation.
- We quantify a speckling model used for assessing framework robustness.
  - Number of clusters chosen from a normal distribution
  - Size of clusters chosen from a categorical distribution

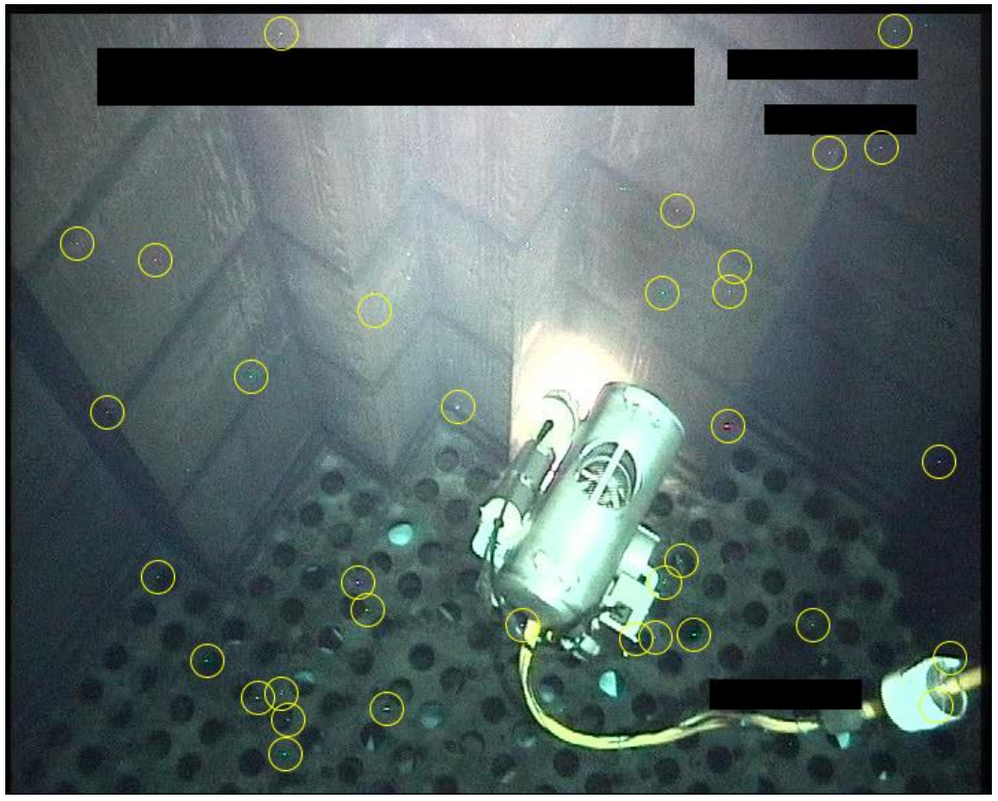

Speckling exhibited in a camera frame.

Outline

Introduction

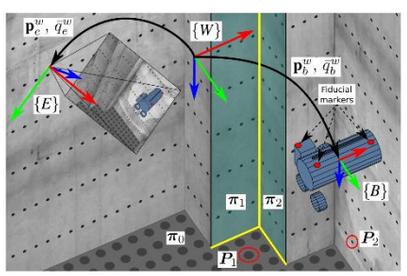

System Models and Methods

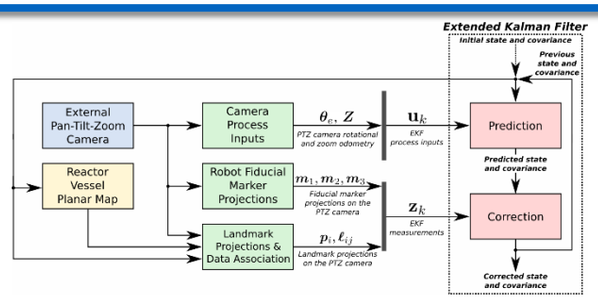

State Estimation and Localization

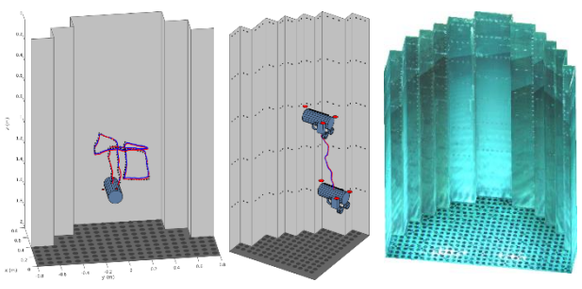

Results

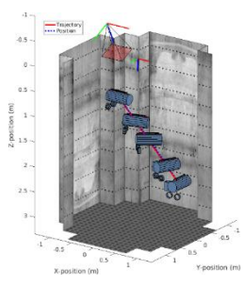

Conclusion and Future Work

State Estimation and Localization

- Non-linear state of the system is estimated using an extended Kalman filter (EKF).
- System is implemented in discrete time to obtain a recursive state estimate.
- The state includes the system (ROV and camera) and the map:

$$\mathbf{X}(t) = [\boxed{\mathbf{X}_S(t)^{\mathrm{T}}}, \mathbf{X}_M{}^{\mathrm{T}}]^{\mathrm{T}}$$

$$\boxed{\begin{gathered}\mathbf{X}_S(t) = [\,\mathbf{p}_b^w(t)^{\mathrm{T}}, \bar{q}_b^w(t)^{\mathrm{T}}, \mathbf{p}_e^{w\mathrm{T}}, \bar{q}_e^w(t)^{\mathrm{T}}, \boldsymbol{f}_e(t)^{\mathrm{T}}\,]^{\mathrm{T}} \\ \boldsymbol{f}_e(t) = [\,f_x(t), f_y(t)\,]^{\mathrm{T}}\end{gathered}}$$

State Estimation and Localization Diagram

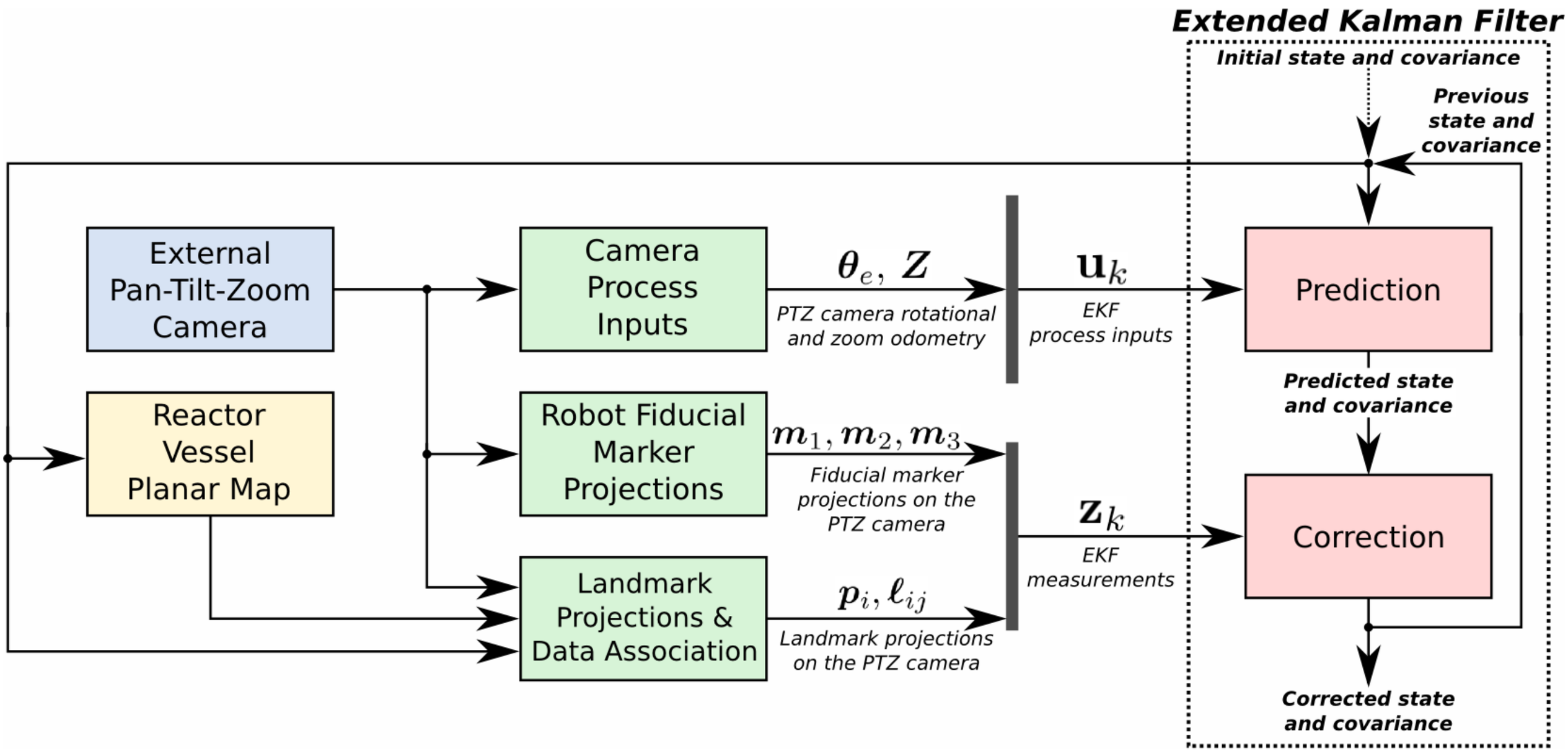

Planar Map

- Minimal representation for EKF
  - Assume baffle plates are orthogonal to core plate

$$\boldsymbol{\pi}_{wall,i} = \begin{bmatrix} \cos\theta_i \\ \sin\theta_i \\ 0 \\ d_i \end{bmatrix} \quad \boldsymbol{\pi}_{floor} = \begin{bmatrix} 0 \\ 0 \\ 1 \\ -h \end{bmatrix} \quad \boldsymbol{\pi}_{top} = \begin{bmatrix} 0 \\ 0 \\ 1 \\ 0 \end{bmatrix}$$

  - 2 DOF for points

$$\boldsymbol{P} = \delta_1 \bar{v}_1 + \delta_2 \bar{v}_2 - \bar{n}d$$

Basis for wall points:

$$\bar{v}_1 = [-\sin\theta,\ \cos\theta,\ 0]^{\mathrm{T}}$$
$$\bar{v}_2 = [0,\ 0,\ 1]^{\mathrm{T}}$$

Basis for floor points:

$$\bar{v}_1 = [1,\ 0,\ 0]^{\mathrm{T}}$$
$$\bar{v}_2 = [0,\ 1,\ 0]^{\mathrm{T}}$$

$$\mathbf{X}_M \in \mathbb{R}^{2N+1+2L}$$
$$\mathbf{X}_M = [\theta_1,\ d_1,\ \ldots,\ \theta_N,\ d_N,\ h,\ \delta_{1,1},\ \delta_{1,2},\ \ldots,\ \delta_{L,1},\ \delta_{L,2}]^{\mathrm{T}}$$

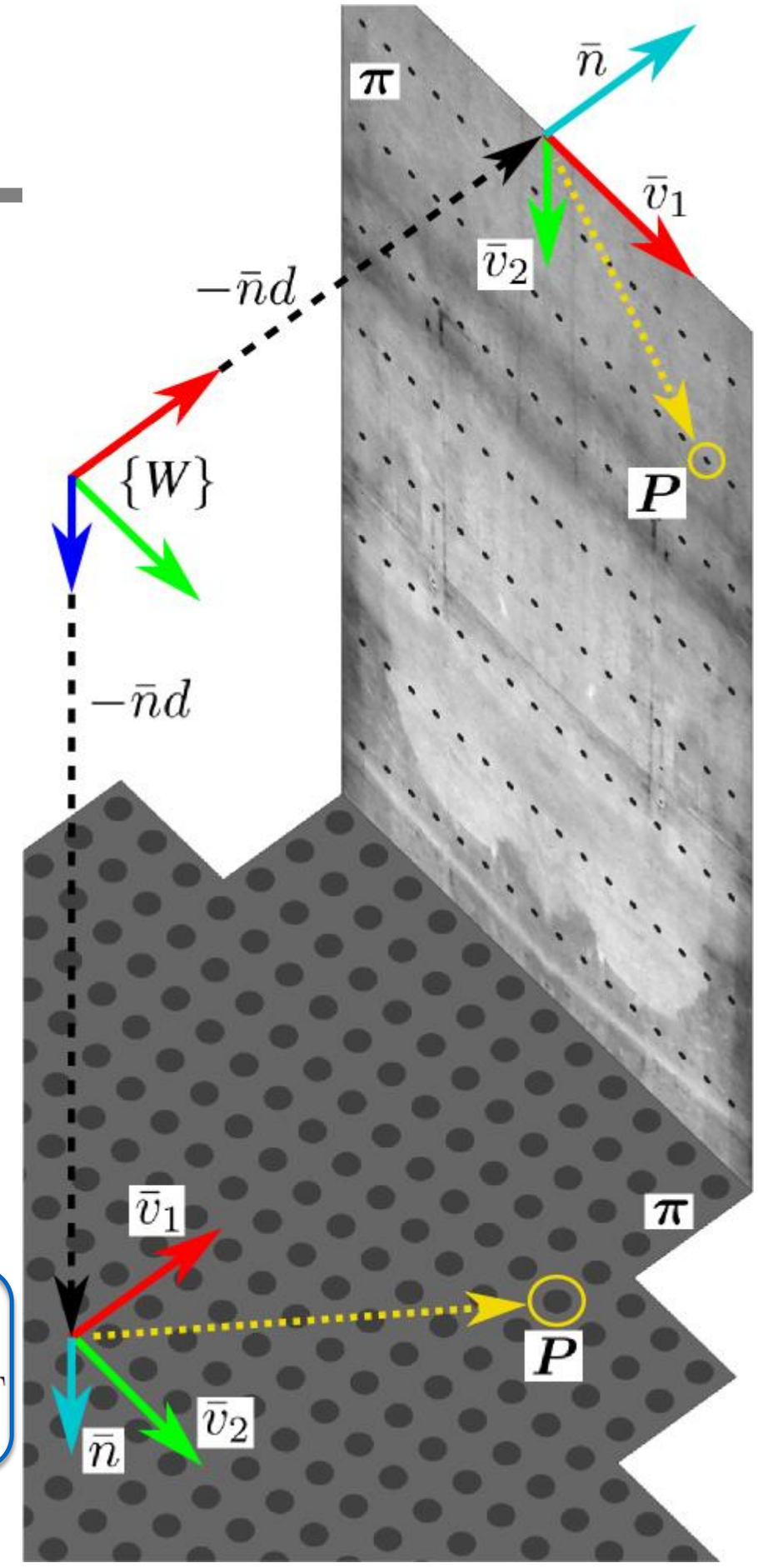

EKF Process Models

- Non-linear process model implemented in discrete time

$$\mathbf{X}_k = g(\mathbf{u}_k,\, \mathbf{X}_{k-1}) + \mathcal{N}(0, Q_k)$$

$$\mathbf{u}_k = \left[\boldsymbol{\theta}_e{}^{\mathrm{T}},\, Z\right]^{\mathrm{T}}$$

- Process inputs
  - ROV process from random walk
  - Rotational odometry

$$\boldsymbol{\theta}_e \in \mathbb{R}^3,\, [\boldsymbol{\theta}_e]_\times \in \mathfrak{so}(3)$$

$$R_e = R(I_{3\times3}, \theta_{k-1}, \phi_{k-1})^{-1} R(I_{3\times3}, \theta_k, \phi_k)$$

  - Zoom scale change

$$Z = \left(\frac{z_k}{z_{k-1}} - 1\right) \qquad z \in \mathbb{R}_{\geq 1}$$

$$g(\mathbf{u},\, \mathbf{X}) = \begin{bmatrix} \mathbf{p}_b^w \\ \bar{q}_b^w \\ \mathbf{p}_e^w \\ ||\, \bar{q}_e^w + \frac{1}{2}\, Q(\boldsymbol{\theta}_e)\, \bar{q}_e^w \,|| \\ (Z+1)\, \boldsymbol{f}_e \\ \mathbf{X}_M \end{bmatrix}$$

EKF Measurement Models

- Two types of measurements:
  1. Camera-to-ROV
     - Marker projections
  2. Camera-to-World
     - Projection of vessel points
       - Projection of wall (baffle plate) landmarks
       - Projection of floor (core plate) landmarks
     - Projection of vessel lines
       - Projection of Plücker lines between adjacent walls (baffle plates)
       - Projection of Plücker lines between wall (baffle plate) and floor (core plate)
       - Projection of Plücker lines between wall (baffle plate) and reactor top rim

$$\mathbf{z} = [\, \mathbf{z}_b^{e\mathrm{T}}, \, \mathbf{z}_e^{w\mathrm{T}} \,]^{\mathrm{T}}$$

$$\hat{\mathbf{z}}_k = h(\mathbf{X}_k) + \mathcal{N}(0, R_k)$$

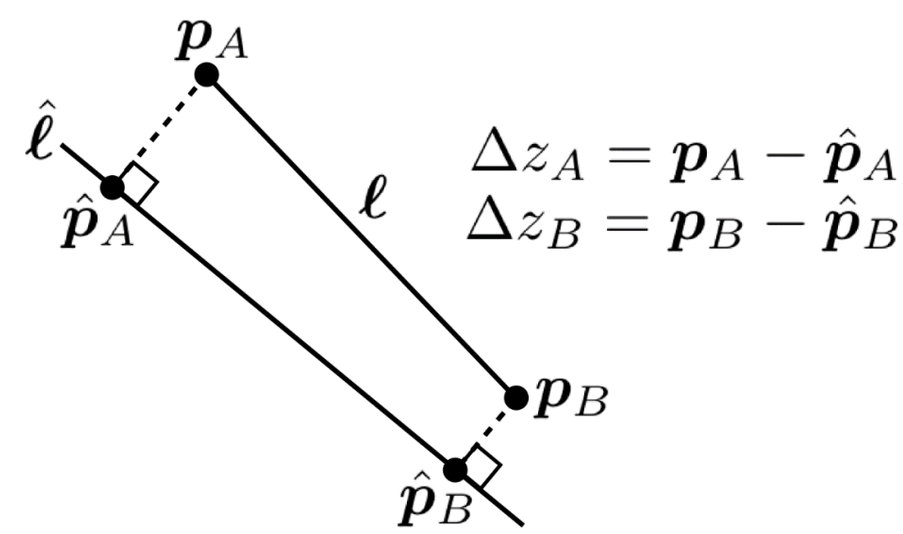

Error function between a predicted line and observed line segment.

EKF Initialization and Data Association

- EKF is initialized from priors on the state, except for the ROV pose.
- Points are detected using blob detection and the Hough transform for circles.[1]
- Lines are detected using the Canny filter[2] and the probabilistic Hough transform for lines.[3]
- Measurements are associated in the image space using a heuristic based on reprojection error between measurement and map estimate.

[1]Yuen et al (1990). [2]Canny (1986).

[3]Matas, Galambos, & Kittler (2000).

Online ROV Initialization

- Determine all possible permutations for the marker association
- For each association:
  - Determine ROV poses that could generate the projections using P3P [4 solutions][1]
  - Remove poses that are not physically viable
  - Remove poses with large ROV roll and pitch
- The remaining poses are assessed a score based on either 1) reprojection error or 2) Mahalanobis distance
- Use pose for initialization if score is below a heuristic threshold and no other viable poses exist

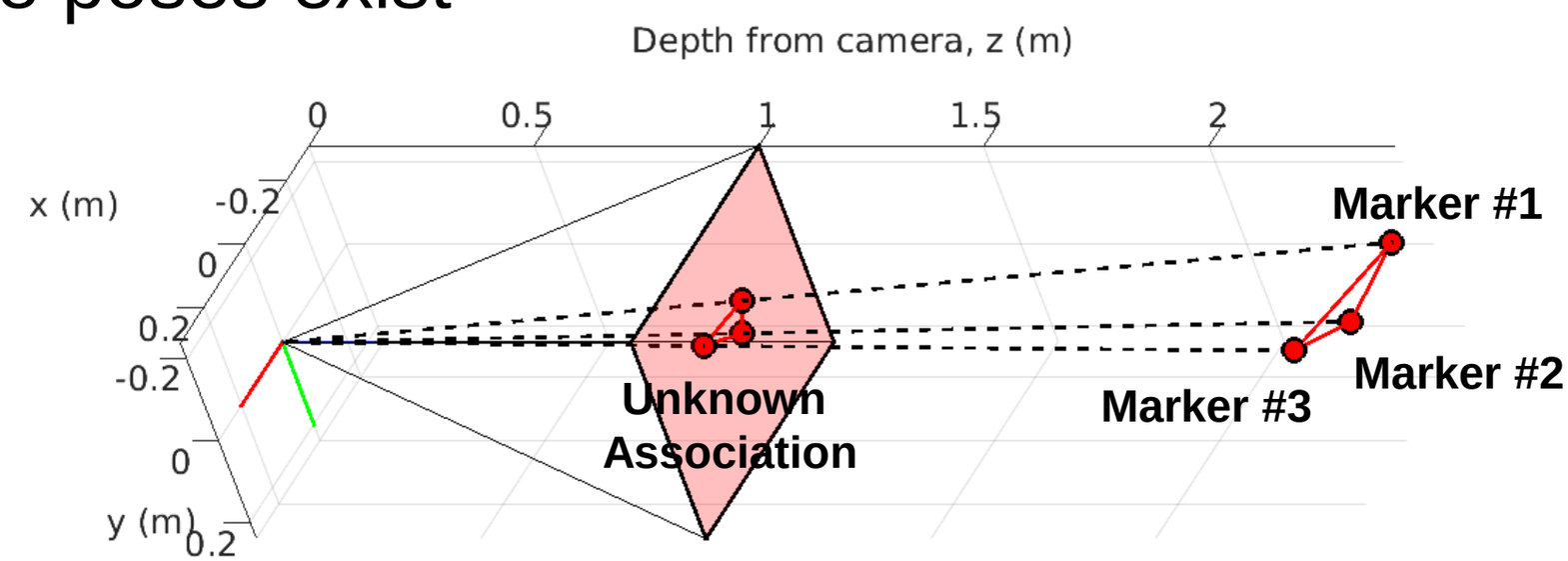

[1]Kneip, Scaramuzza, & Siegwart (2011).

Outline

Introduction

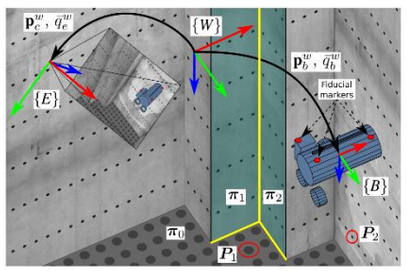

System Models and Methods

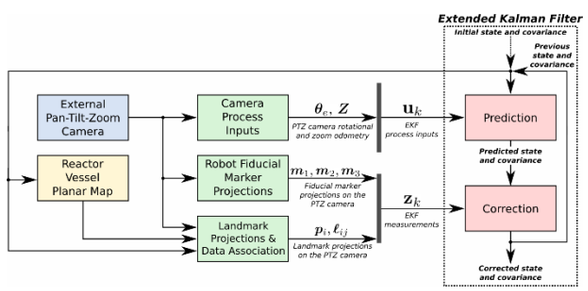

State Estimation and Localization

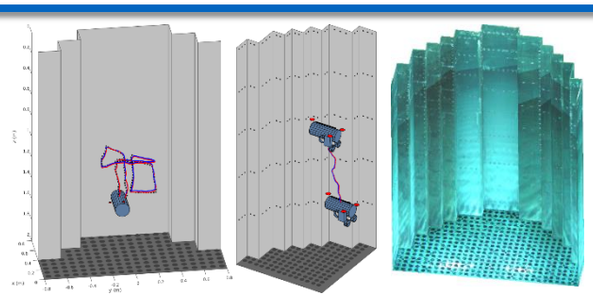

Results

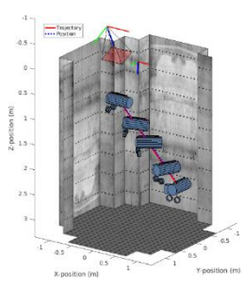

Conclusion and Future Work

Progression of Experiments

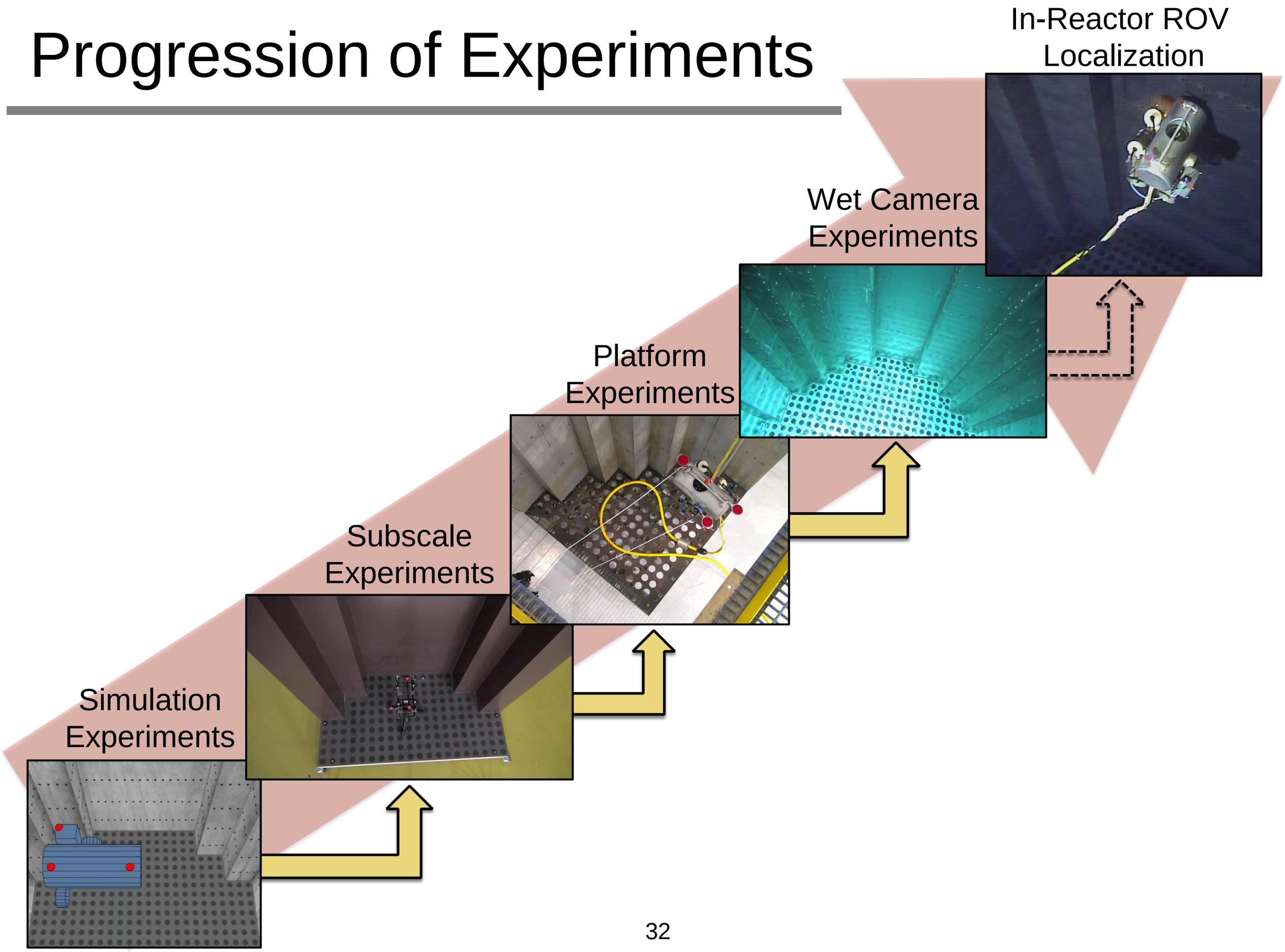

Description of Experiments

- Simulation Experiments
- Subscale and Platform Experiments in Dry Setting
  - Tests of ROV localization
  - Experiments were repeated twice
    - “Clean”
    - “Degraded” --- artificial speckling and color attenuation
- Camera Experiments in Wet Setting
  - Underwater footage with PTZ camera validated system
  - Dense reconstruction for visual inspection

Simulation Experiments

- ROV position estimates under 6 cm in *x-y*, 10 cm in *z*
- ROV yaw estimate under 2 deg
- Successful tracking of focal length components during zoom

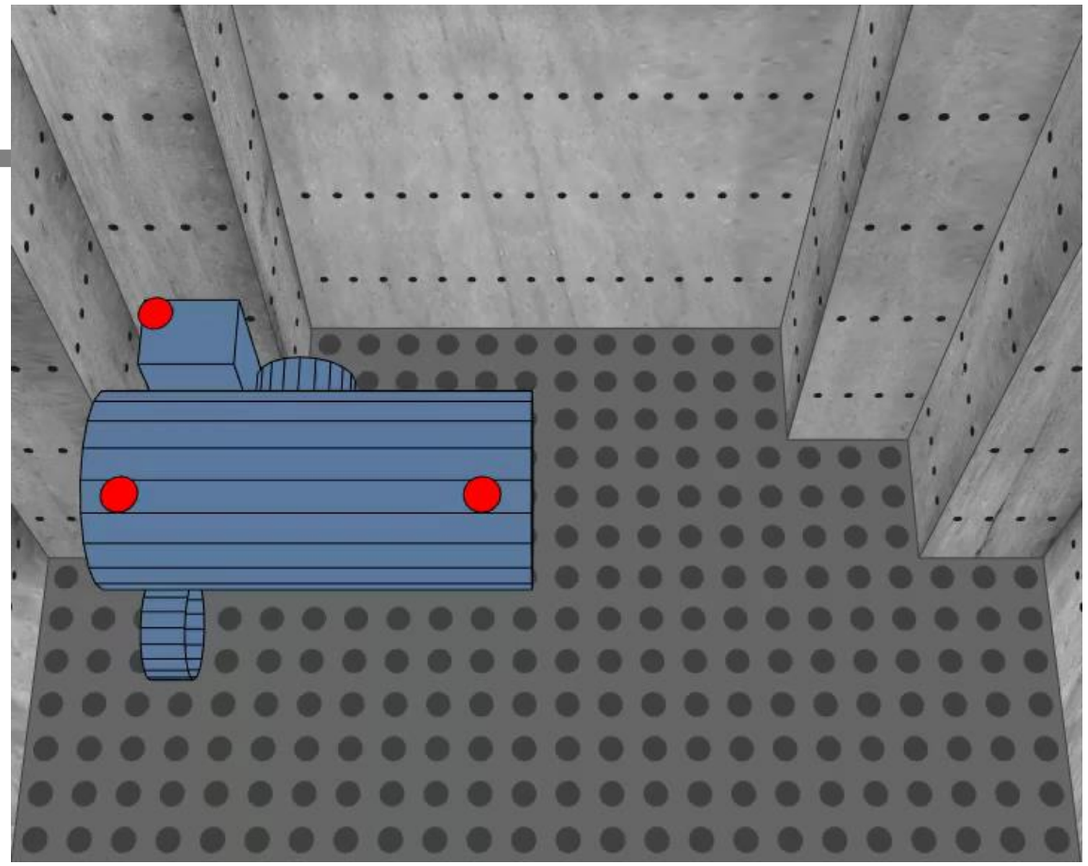

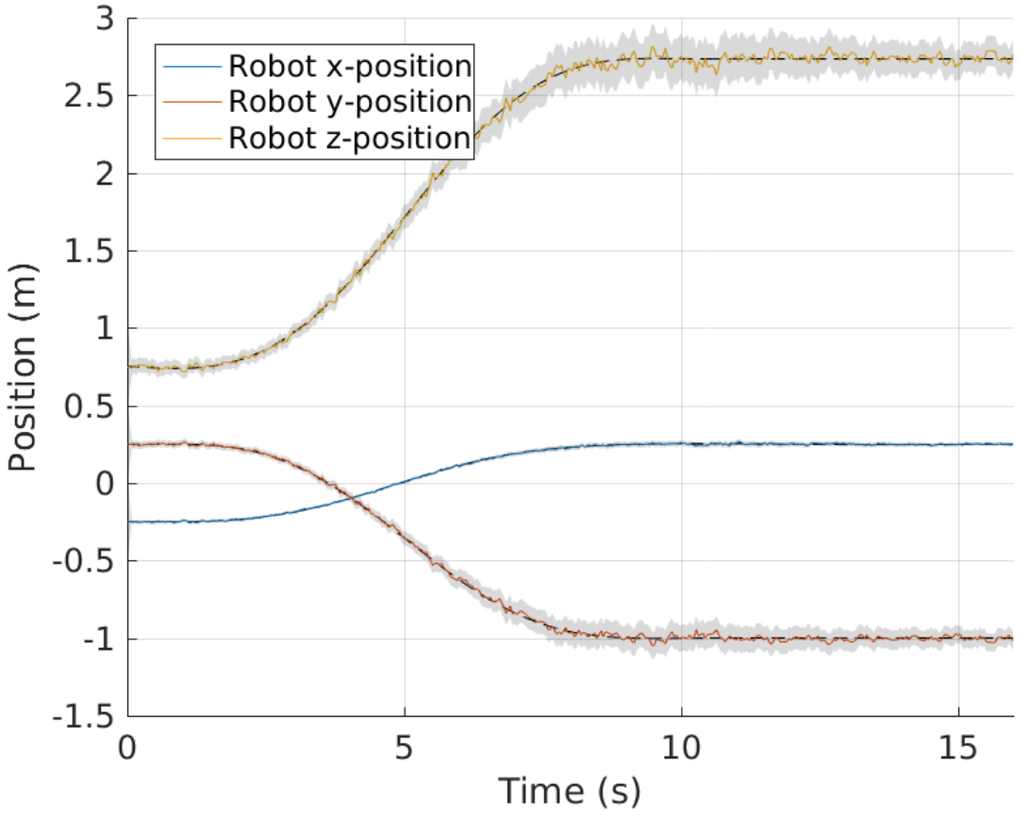

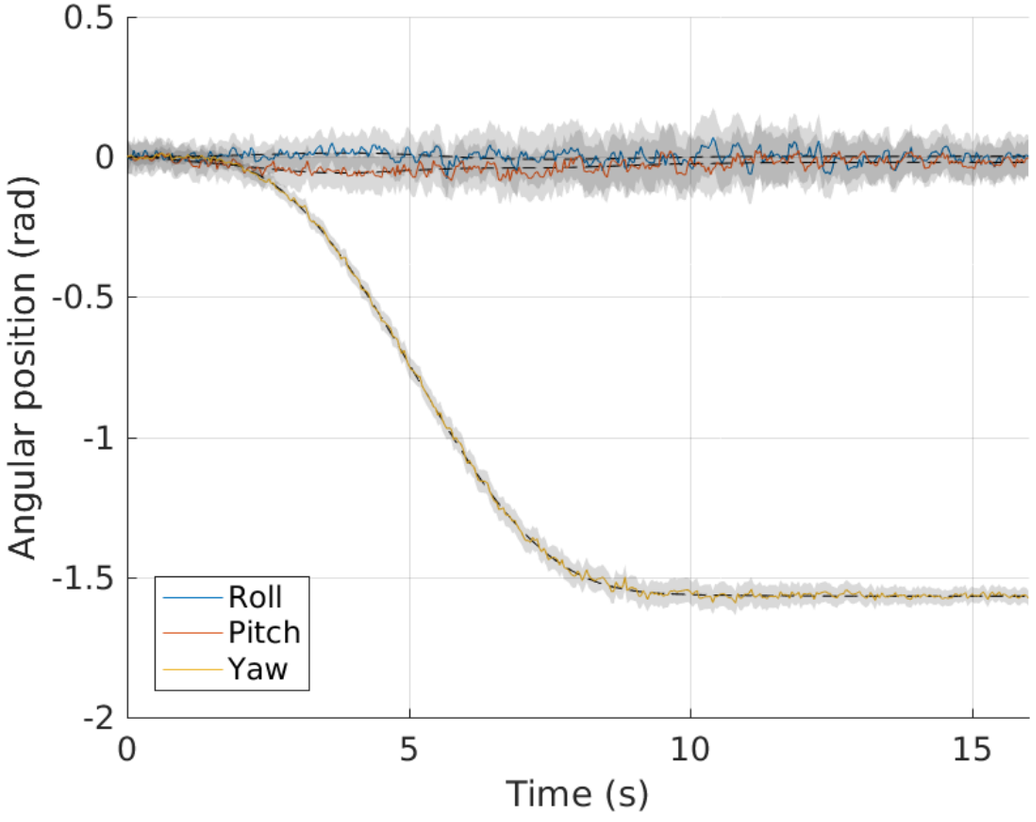

Online ROV Initialization

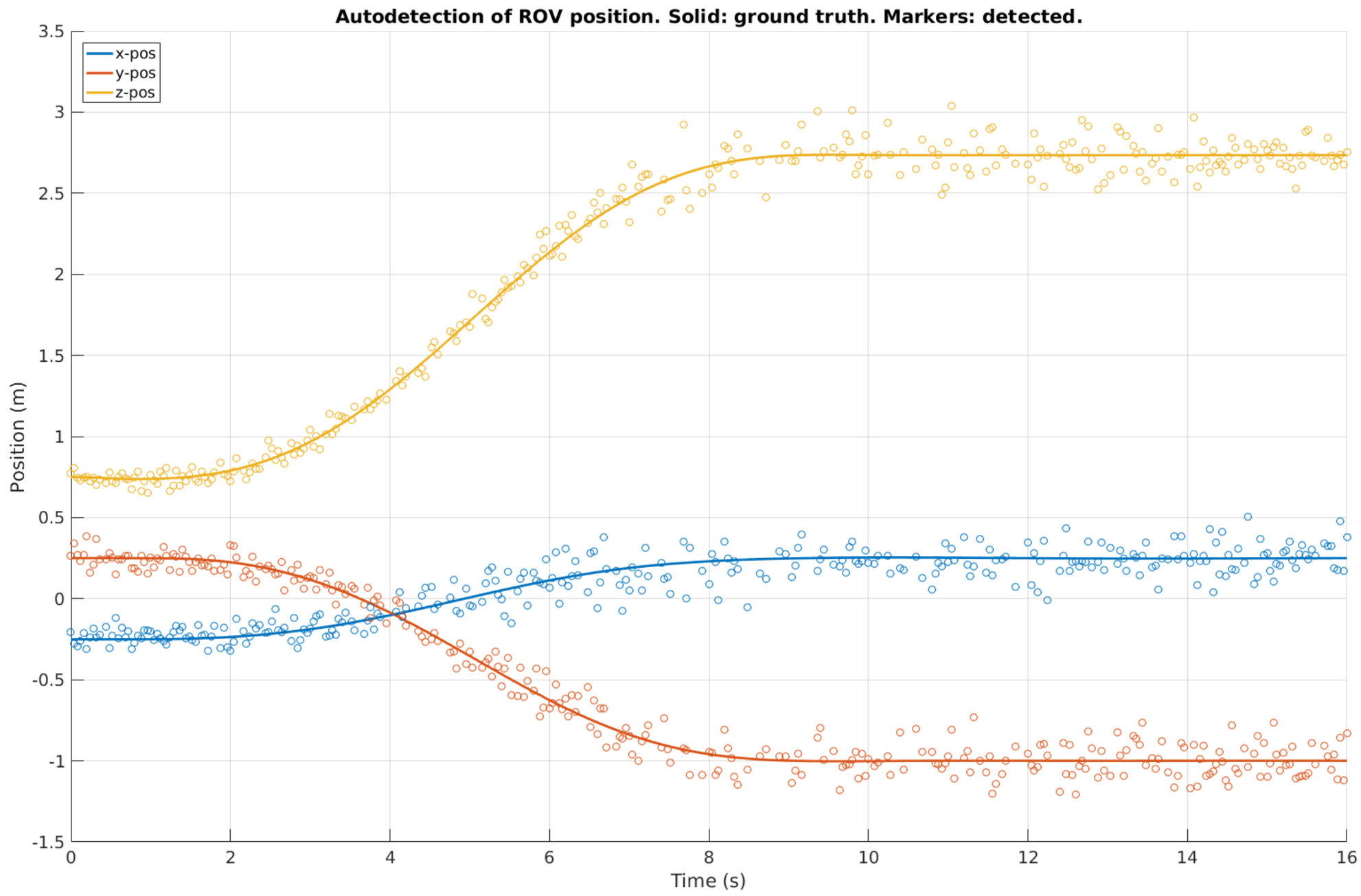

- Despite large added noise to state, obtained an estimate for ROV pose in 95% of the cases

Subscale Experiments

- A subscale mockup reactor allows for conducting camera experiments
- VICON motion capture

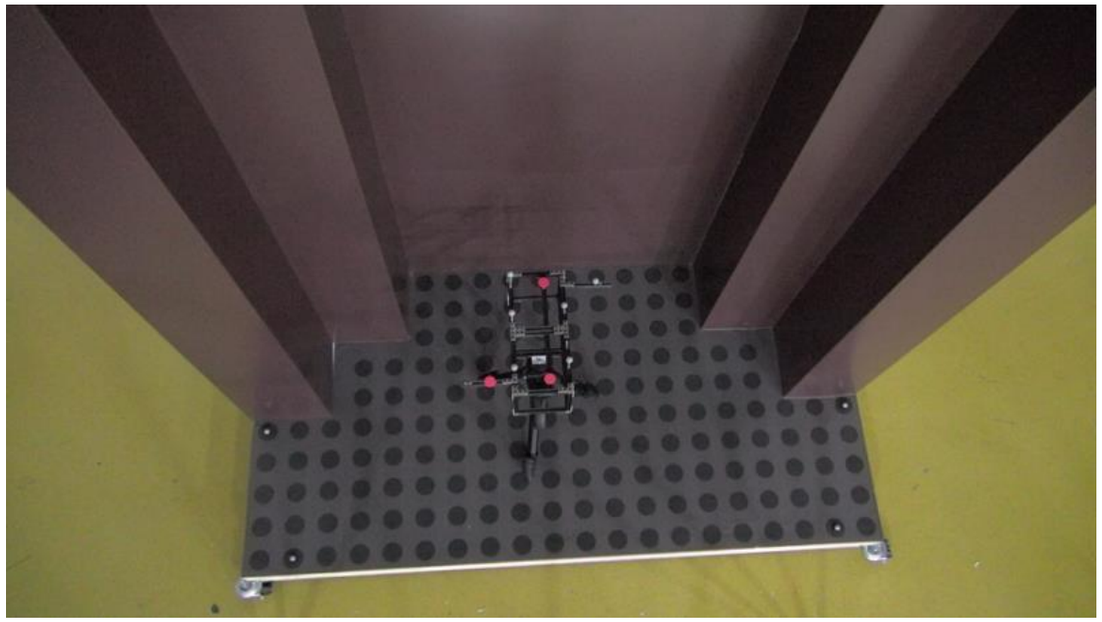

Subscale Experiments: Clean

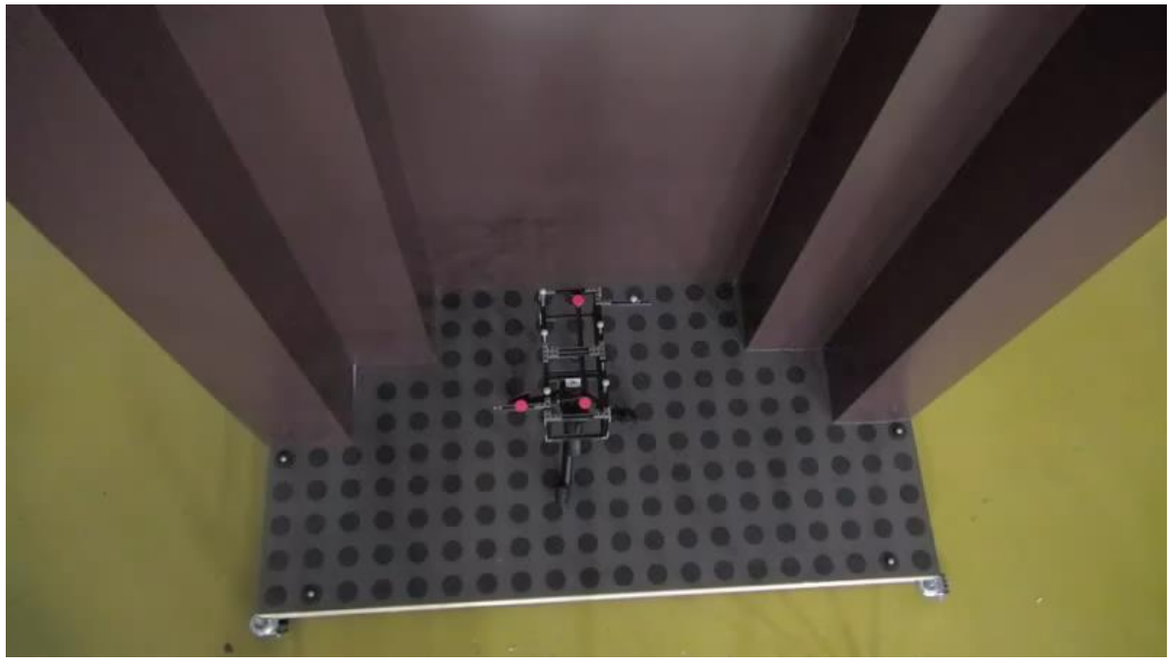

PTZ footage

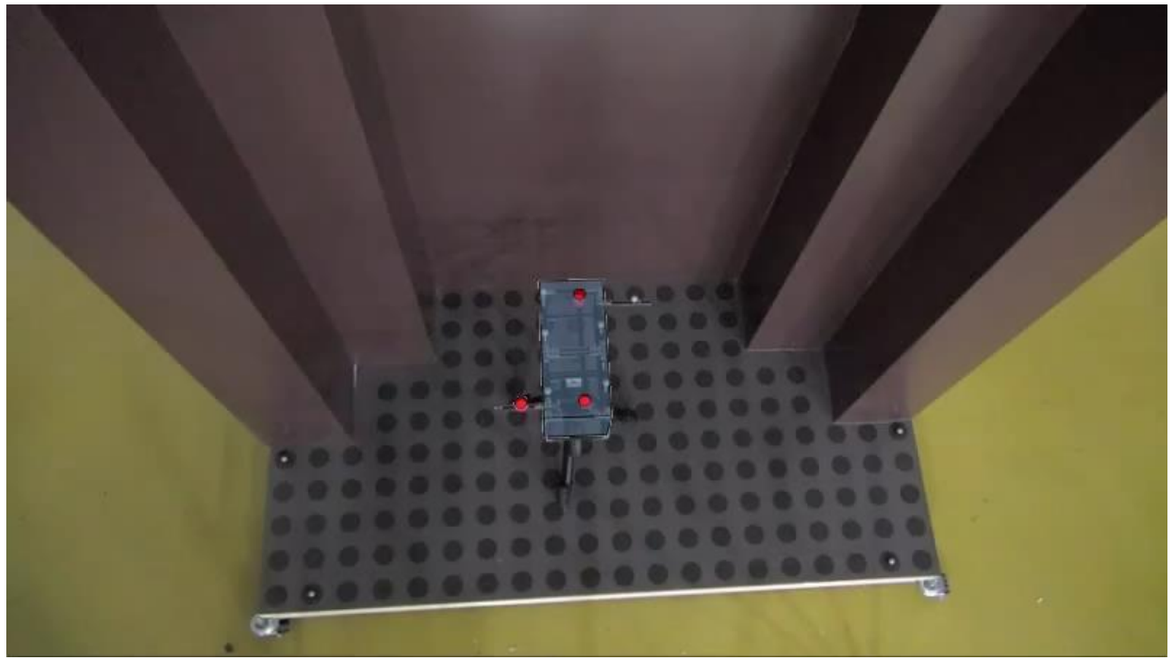

Estimated ROV pose

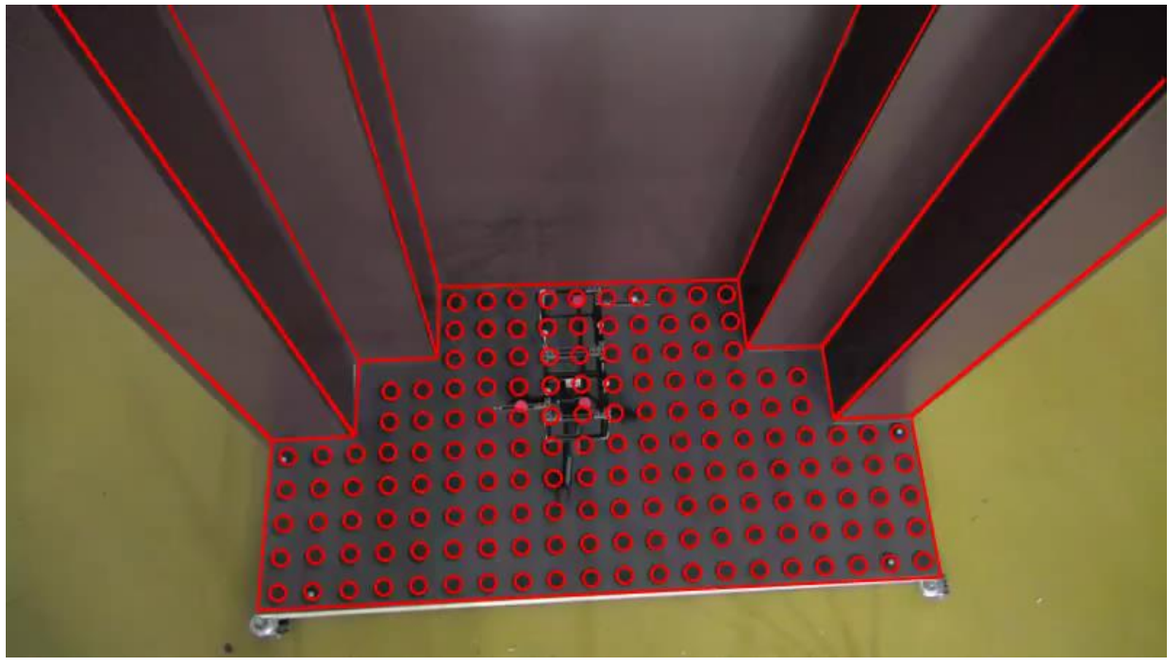

Map overlay

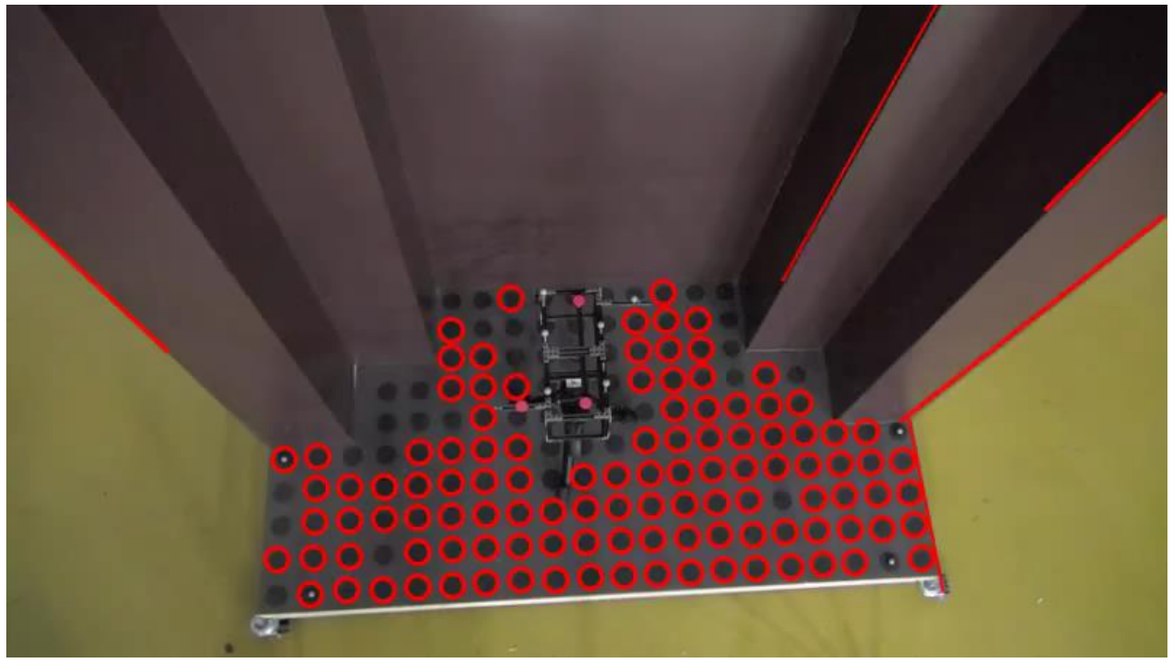

Associated landmarks

Subscale Experiments: Degraded

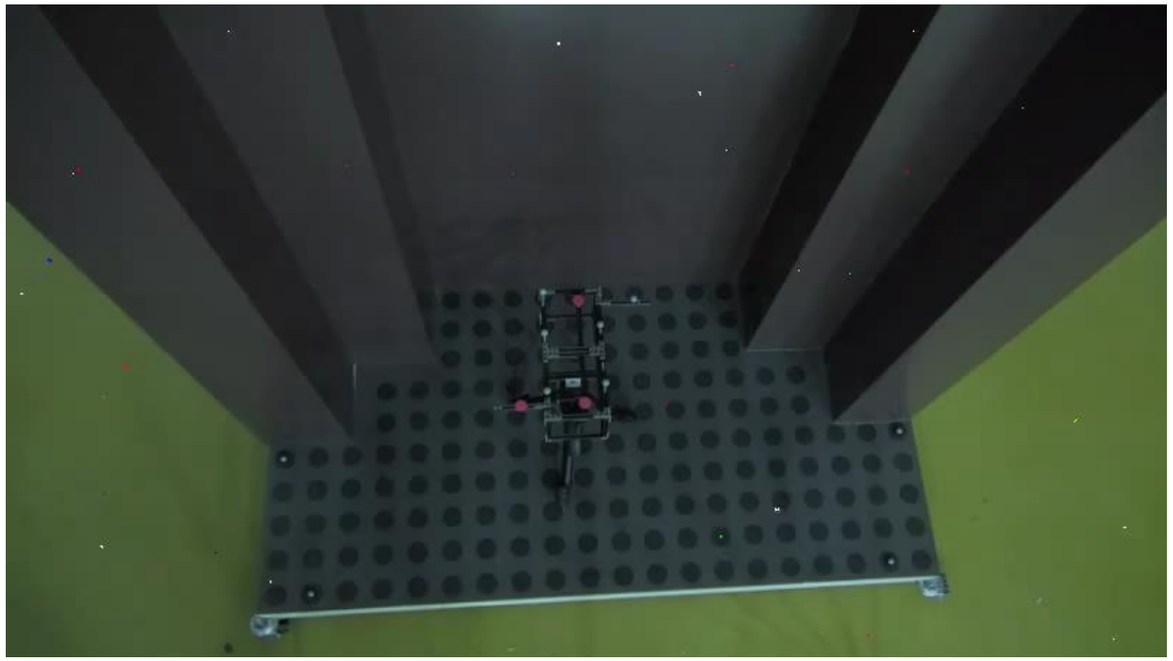

PTZ footage

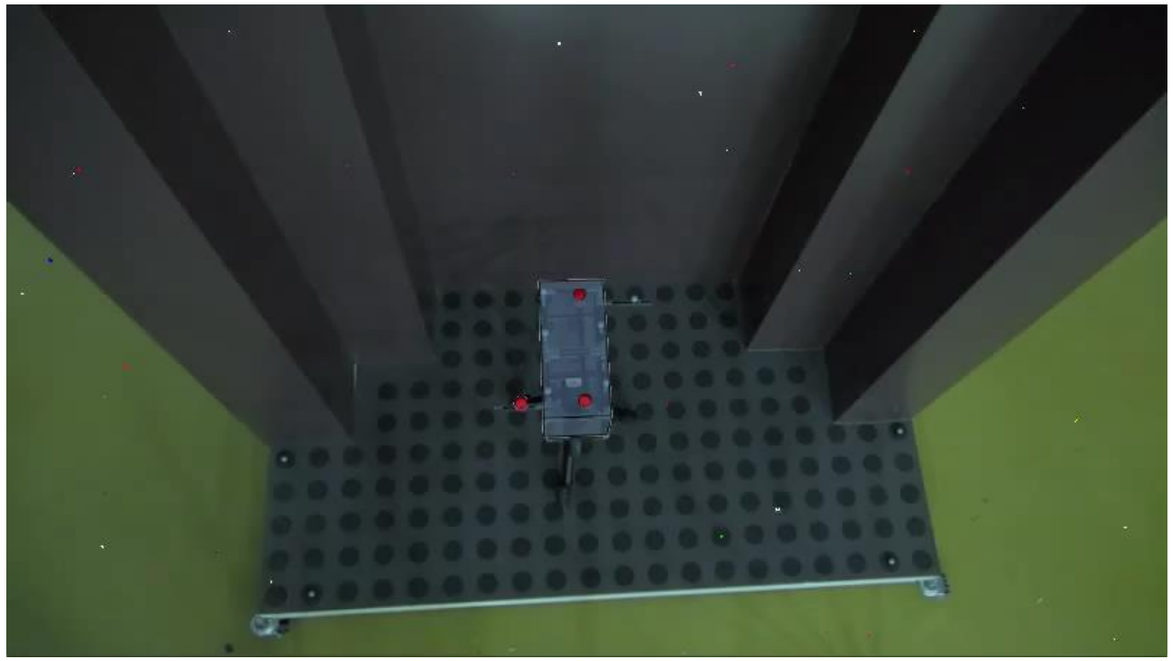

Estimated ROV pose

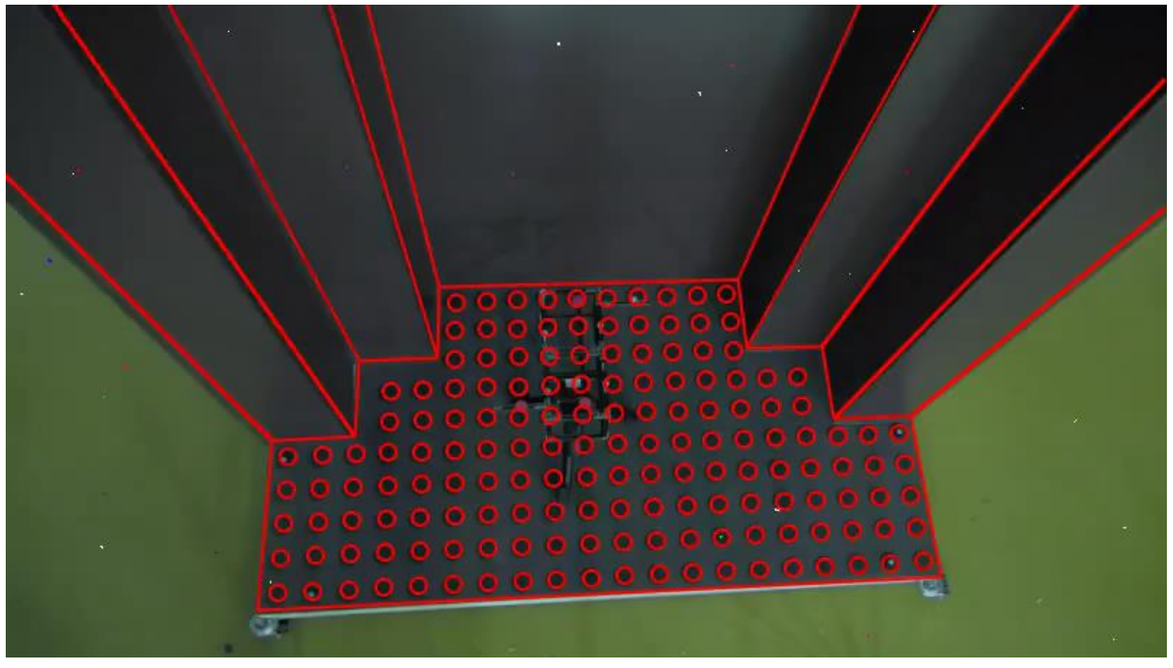

Map overlay

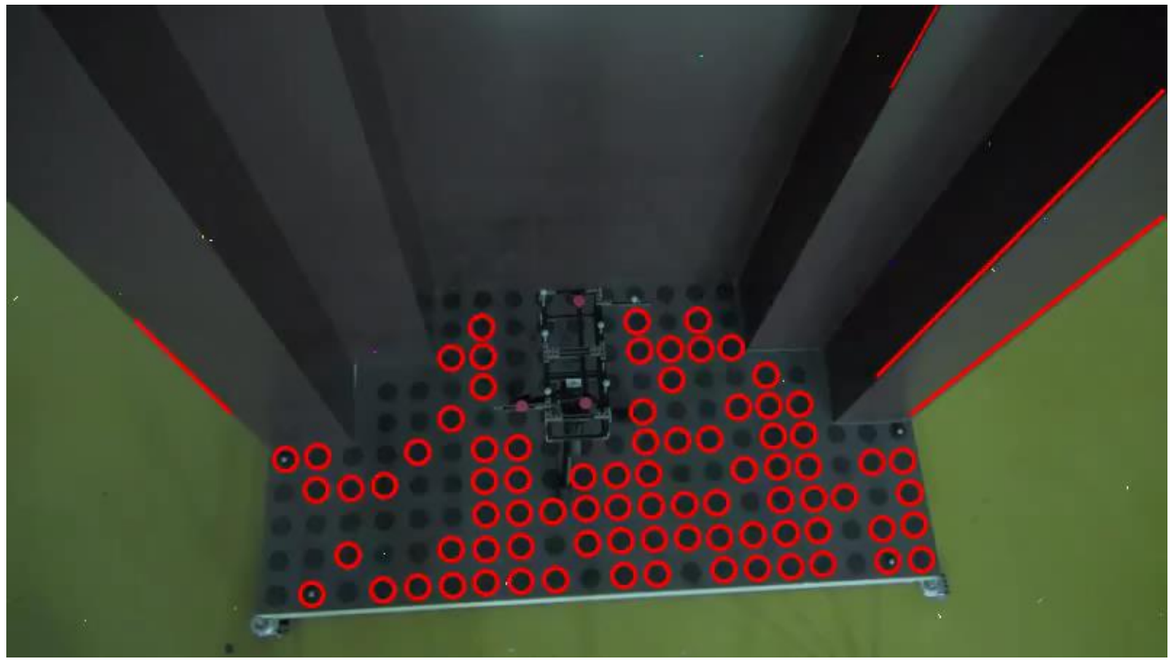

Associated landmarks

Subscale Experiments

- Uncertainty less than 4.5 cm in ROV *x*, 2 cm in ROV *y*, and 10 cm in ROV *z*
- Slight decrease in accuracy due to degradation

Parameter	Value (Clean)	Value (Degraded)
Accuracy (MSE), m^2 or rad^2		
x_b^w	2.7515e−4	2.8637e−4
y_b^w	3.0282e−4	3.0809e−4
z_b^w	1.6192e−3	1.6982e−3
θ_e^w	3.6473e−4	3.7681e−4
ϕ_e^w	1.1025e−3	1.2869e−3
ψ_e^w	6.0344e−4	6.7328e−4
Uncertainty ($\pm 3\sigma$), m or rad		
Robot, $\{B\}$		
x_b^w	0.0435	0.0434
y_b^w	0.0174	0.0175
z_b^w	0.0961	0.0960
θ_b^w	0.1361	0.1358
ϕ_b^w	0.1101	0.1118
ψ_b^w	0.0527	0.0520
External camera, $\{E\}$		
x_e^w	0.0028	0.0037
y_e^w	0.0021	0.0034
z_e^w	0.0393	0.0424
θ_e^w	0.0053	0.0056
ϕ_e^w	0.0048	0.0051
ψ_e^w	0.0162	0.0172

Uncertainty in subscale experiments.

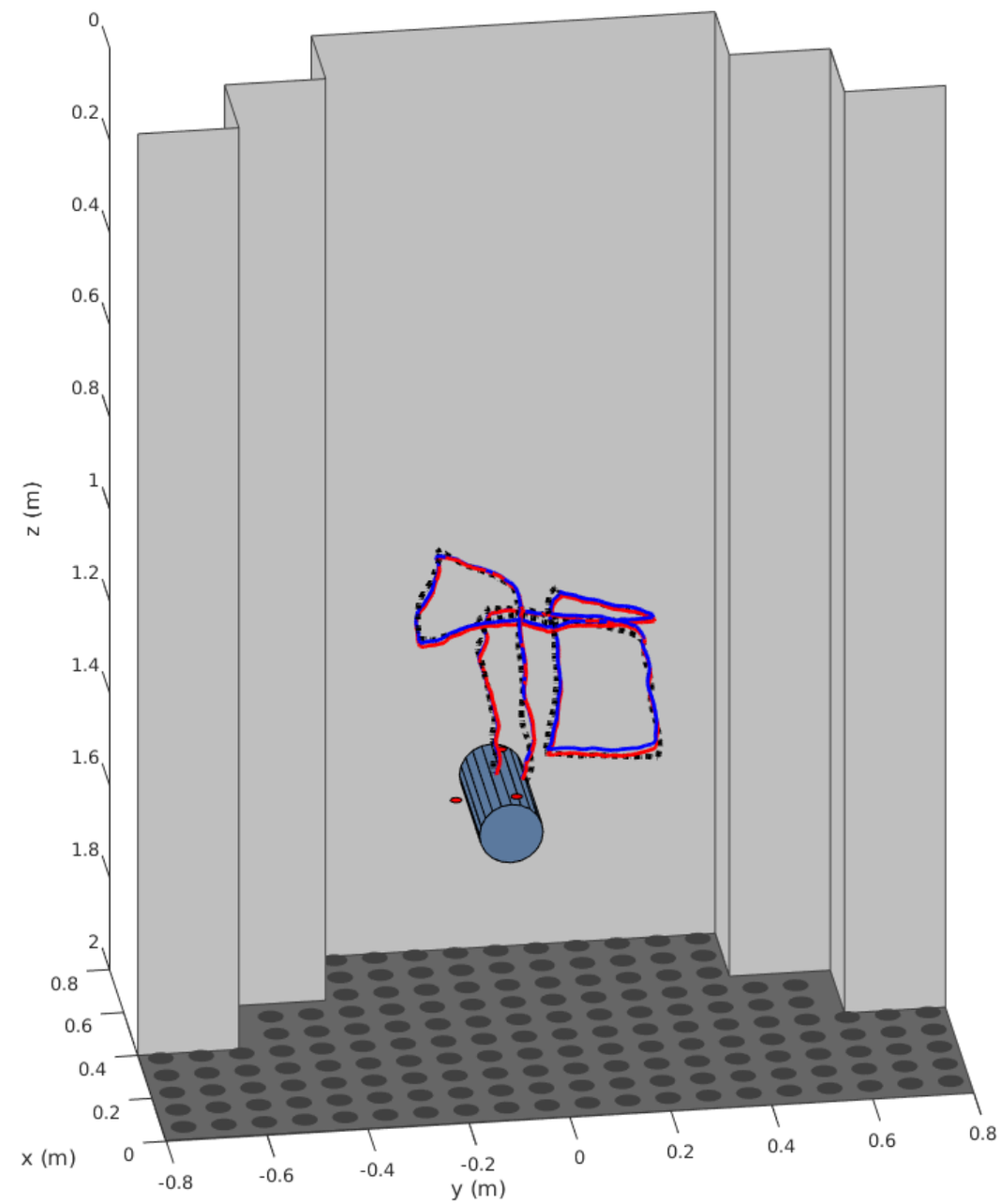

ROV path:
black (ground truth),
red (est., clean), blue (est., degraded)

Platform Experiments

- Motions tests were also conducted with the ROV platform in a dry setting
- Reactor mockup has wall landmarks

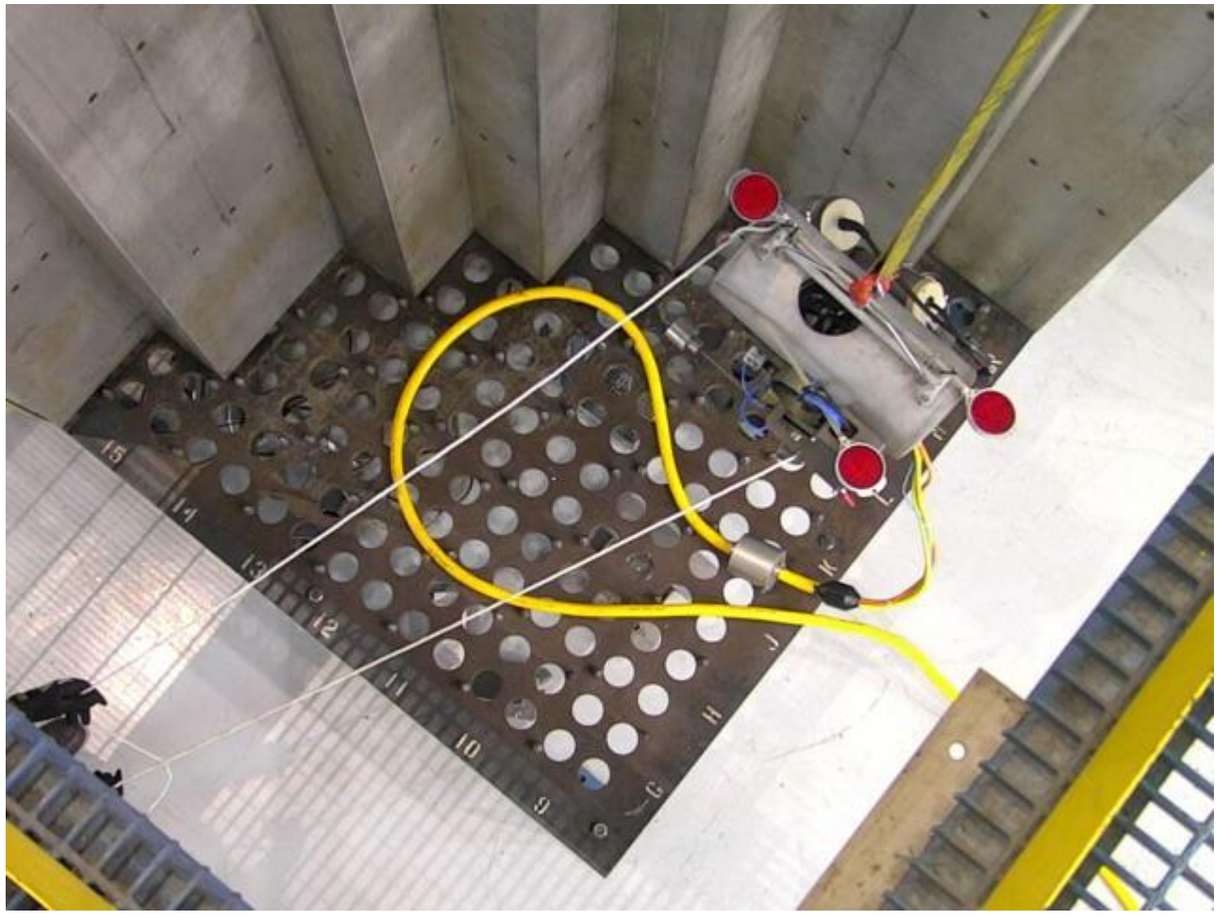

Platform Experiments: Clean

PTZ footage

Estimated ROV pose

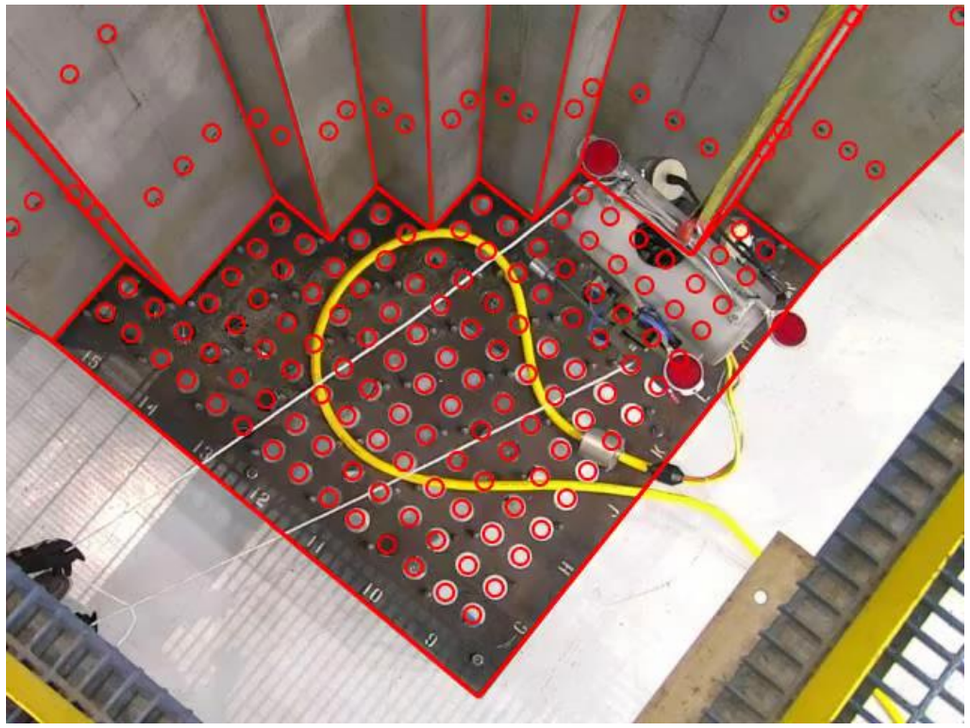

Map overlay

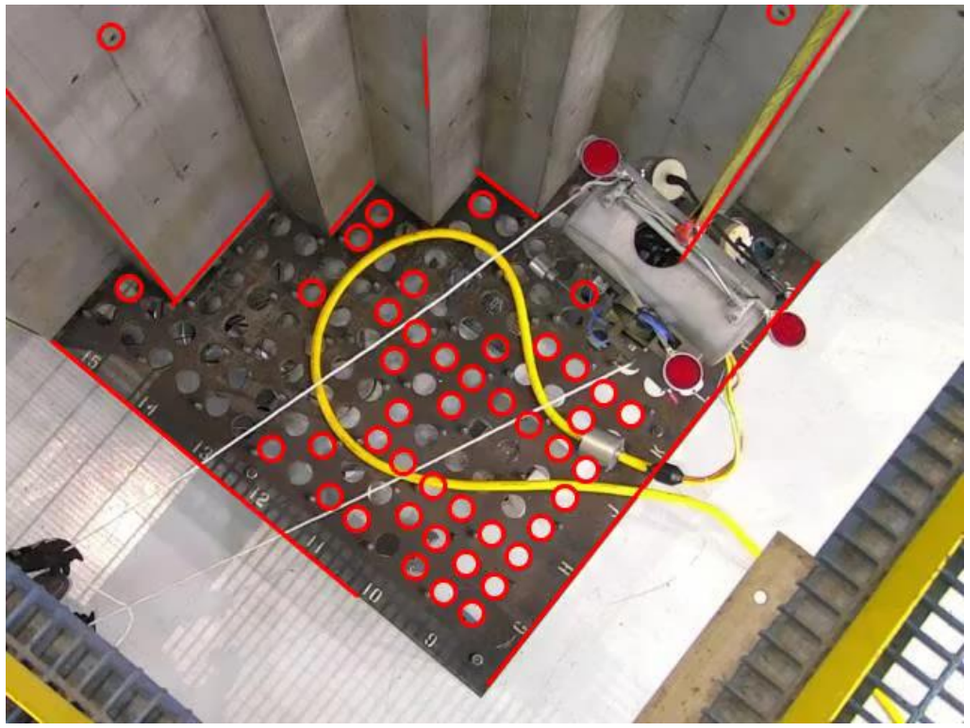

Associated landmarks

Platform Experiments: Degraded

PTZ footage

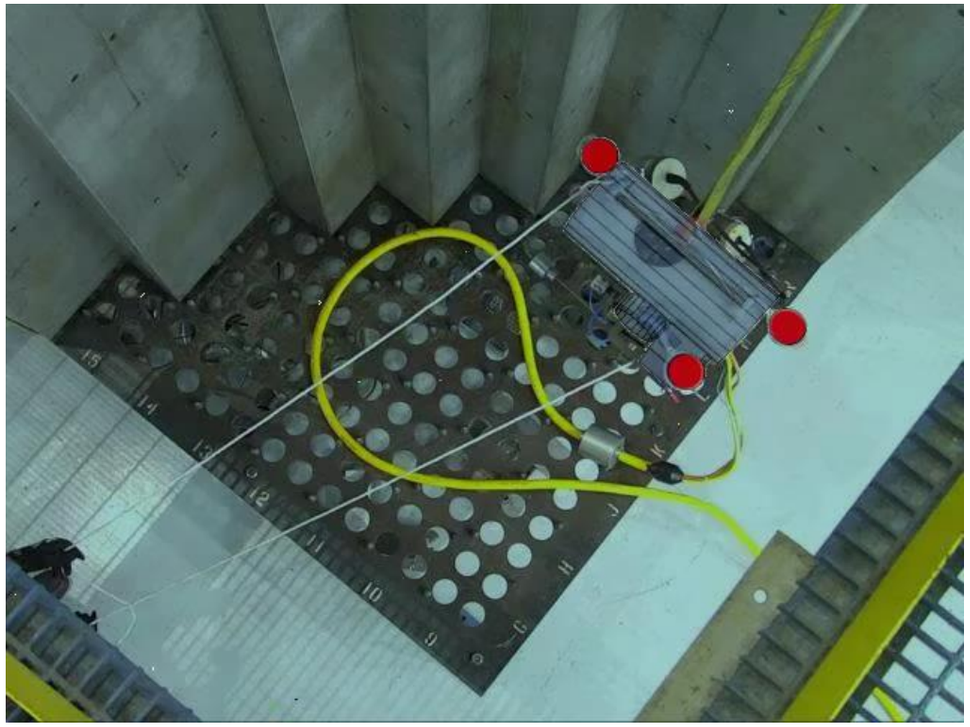

Estimated ROV pose

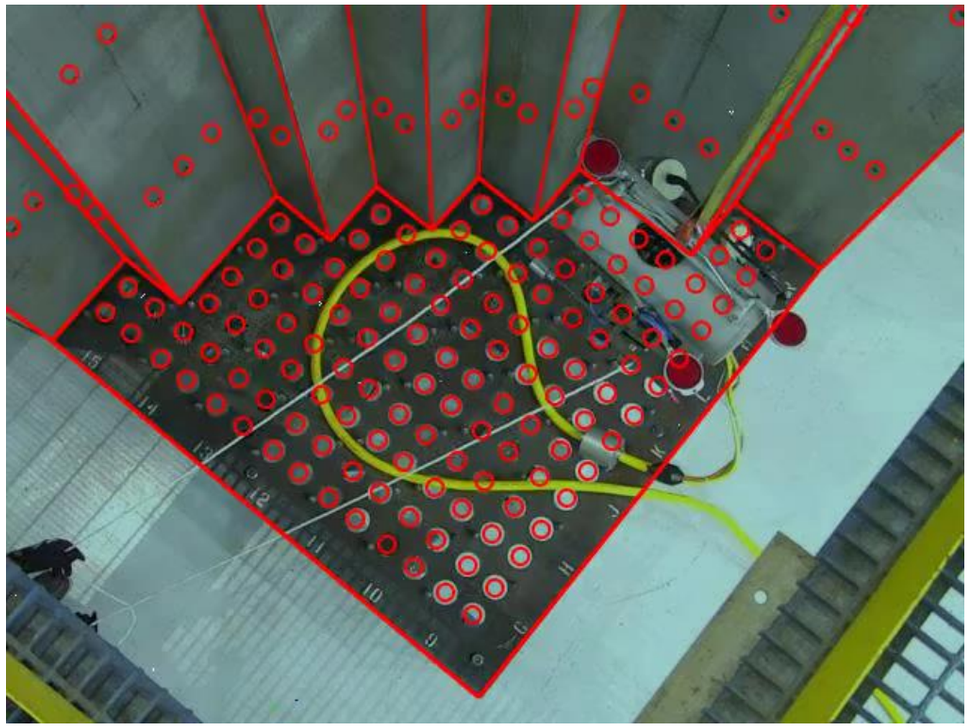

Map overlay

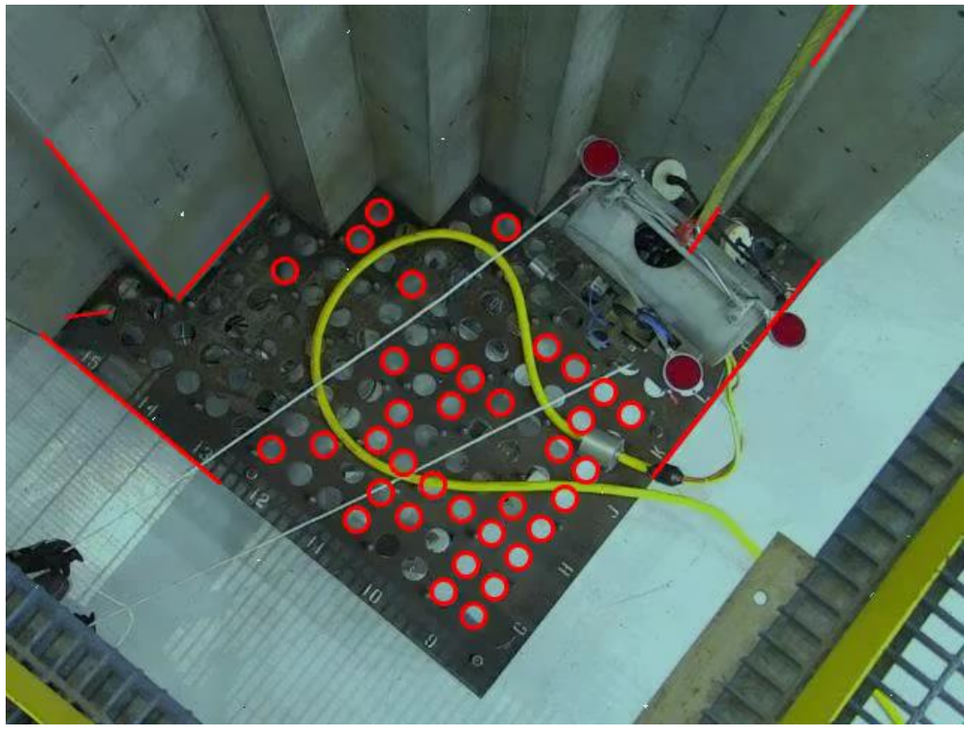

Associated landmarks

Platform Experiments

- Less than 2 cm uncertainty in ROV *x* and *y*
- Less than 2.5 cm uncertainty in ROV *z*
- Framework is robust to image degradation
- Overall less uncertainty than in subscale experiments

Parameter	Value (Clean)	Value (Degraded)
Uncertainty ($\pm 3\sigma$), m or rad		
Robot, $\{B\}$		
x_b^w	0.0085	0.0084
y_b^w	0.0161	0.0162
z_b^w	0.0241	0.0237
θ_b^w	0.0687	0.0727
ϕ_b^w	0.0395	0.0406
ψ_b^w	0.0214	0.0225
External camera, $\{E\}$		
x_e^w	0.0031	0.0031
y_e^w	0.0036	0.0036
z_e^w	0.0166	0.0190
θ_e^w	0.0035	0.0039
ϕ_e^w	0.0033	0.0035
ψ_e^w	0.0092	0.0097

Uncertainty in platform experiments.

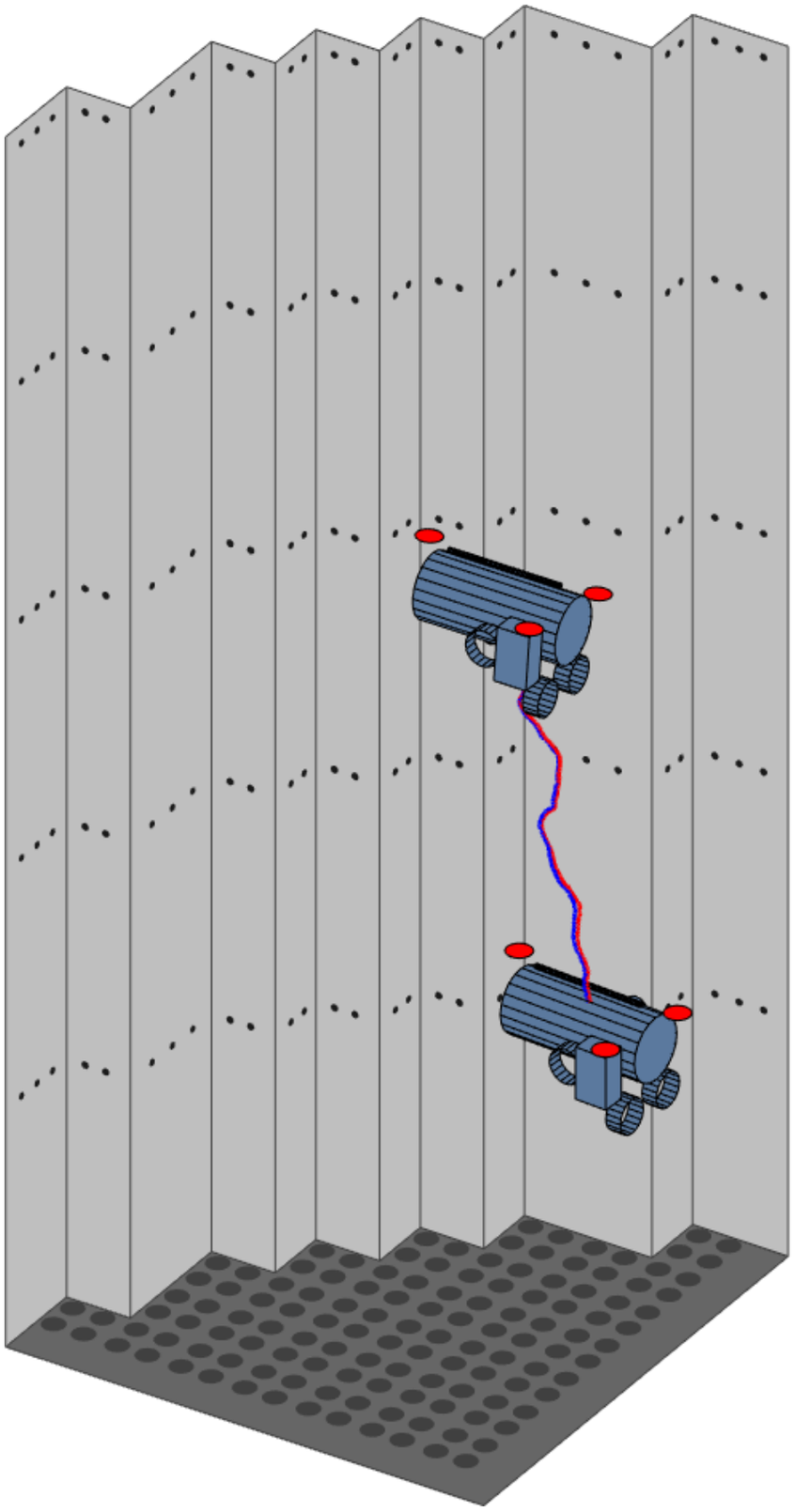

Estimated ROV path:
red (clean), blue (degraded)

Visual Inspection: Reactor Mosaics

- Generation of high fidelity mosaics for reactor visual inspection

$$\widetilde{\boldsymbol{x}}_j = H\,\widetilde{\boldsymbol{x}}_i$$

$$H = K\,R_{rel}\,K^{-1}$$

$$R_{rel} = R_j^w\,(R_i^w)^{-1}$$

$$R_i^w = R(R_{scene}, \theta_i, \phi_i)$$

$$R_j^w = R(R_{scene}, \theta_j, \phi_j)$$

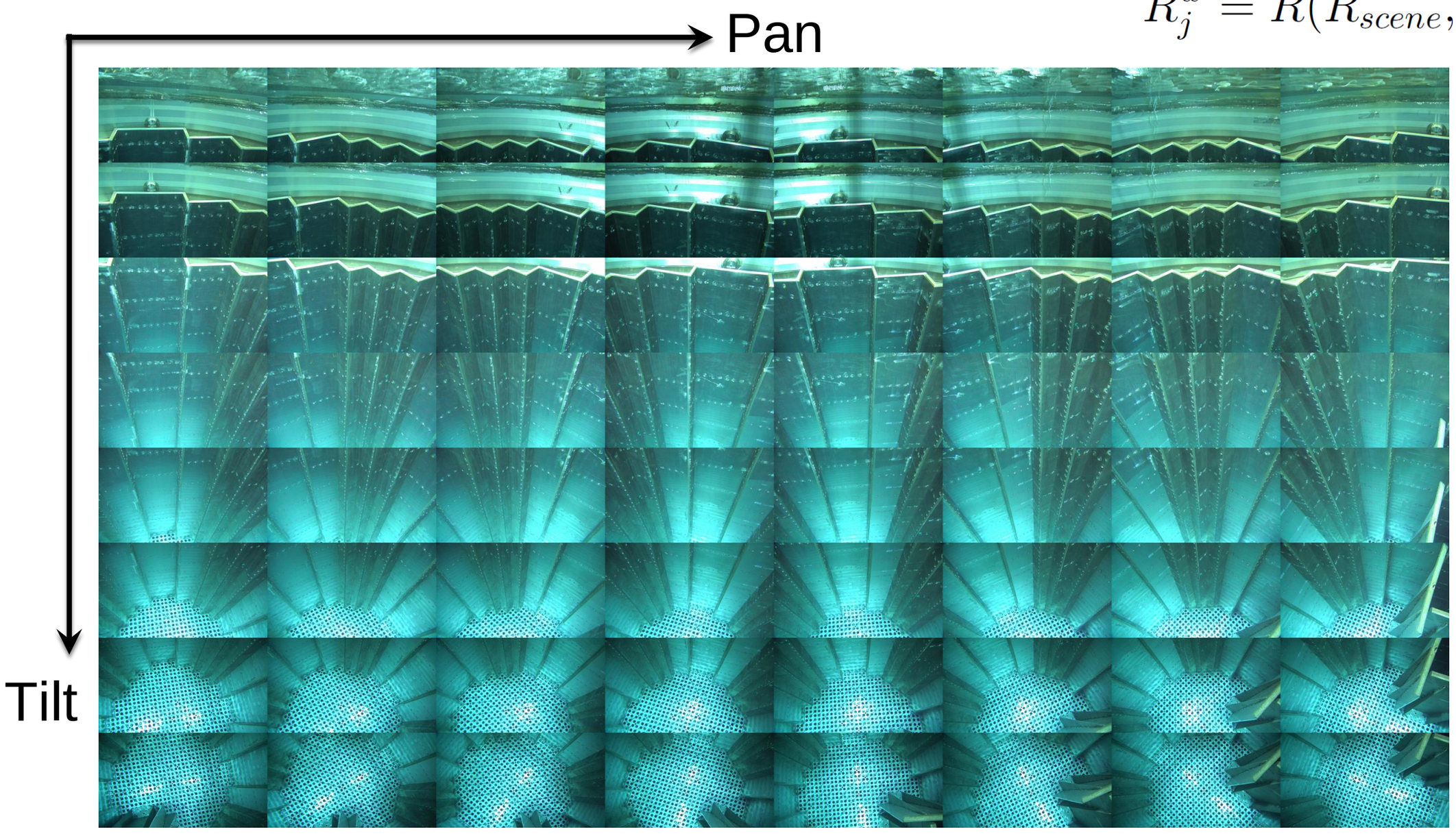

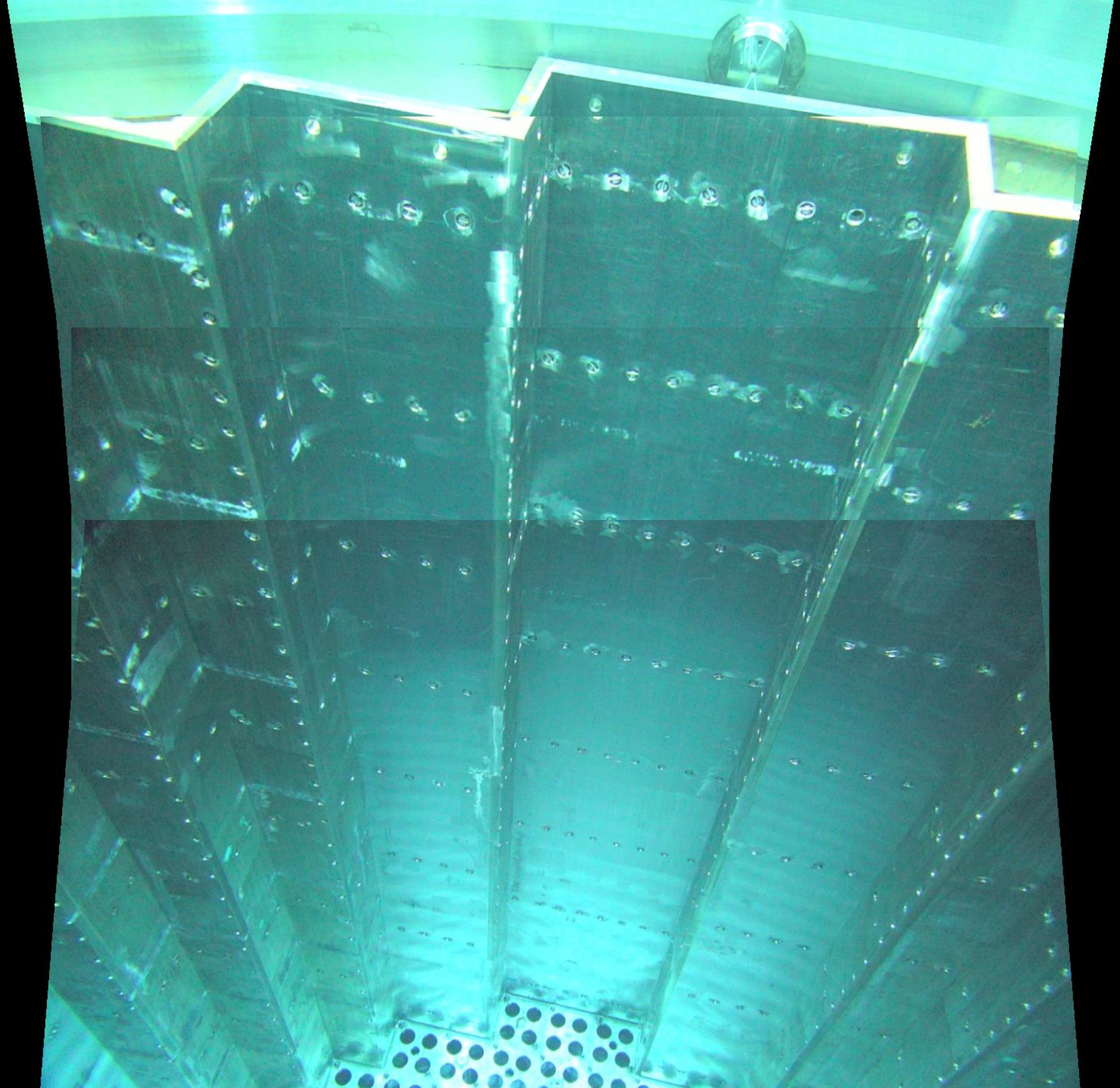

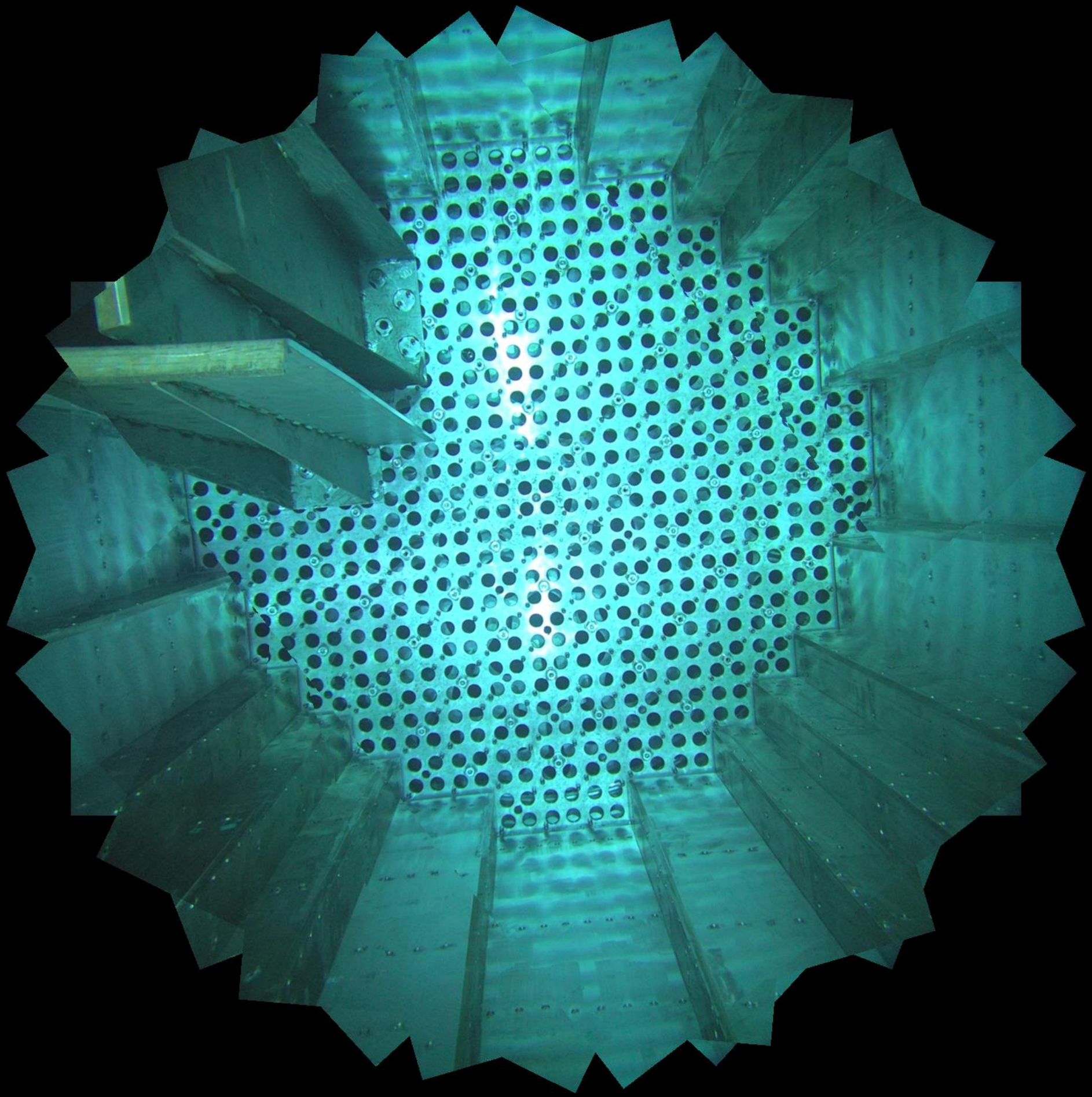

Visual Inspection: Dense Reconstructions

- Dense reconstruction of lower core creates new avenues for inspection
- 3D homography maps from mosaic to a reactor plane

$$\widetilde{\boldsymbol{X}}' = H_{3d}\,\widetilde{\boldsymbol{X}}$$

$$\widetilde{\boldsymbol{X}} = [\,u,\ v,\ 0,\ 1\,]^{\mathrm{T}}$$

$$\widetilde{\boldsymbol{X}}' = [\,x,\ y,\ z,\ 1\,]^{\mathrm{T}}$$

Image frame from higher zoom level

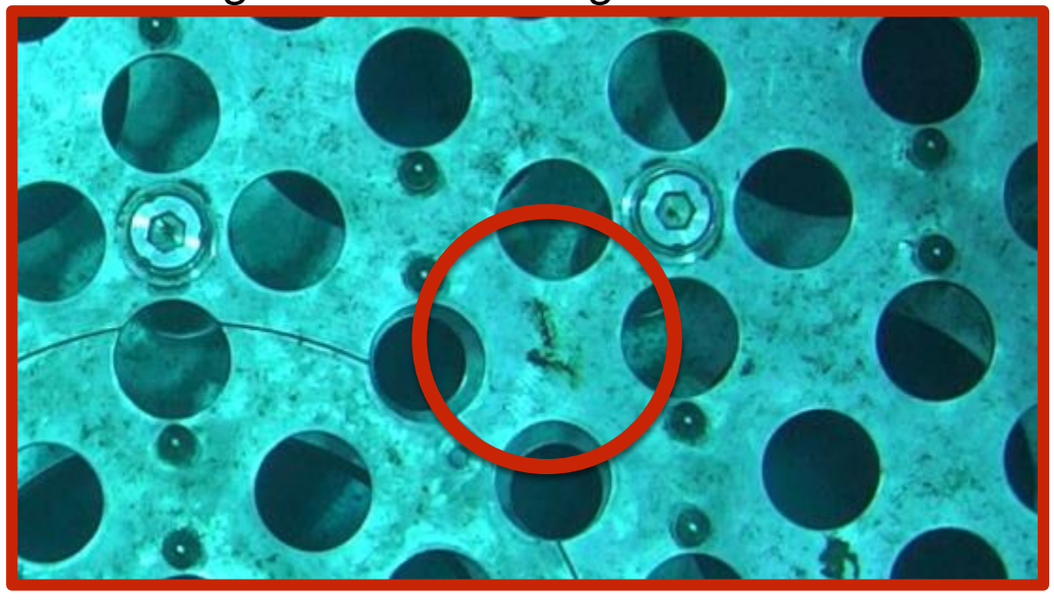

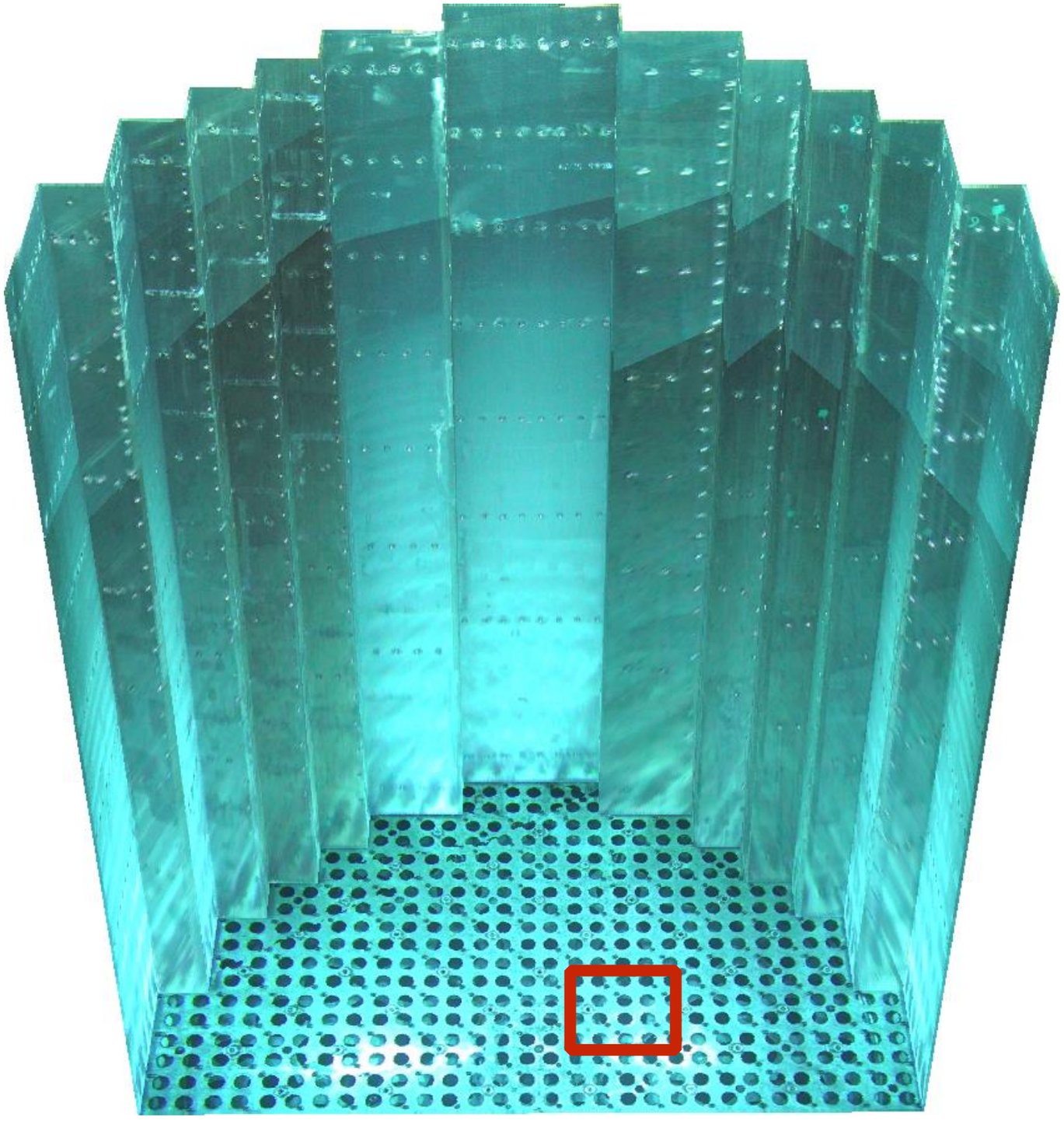

Outline

Introduction

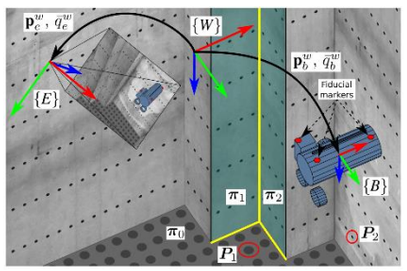

System Models and Methods

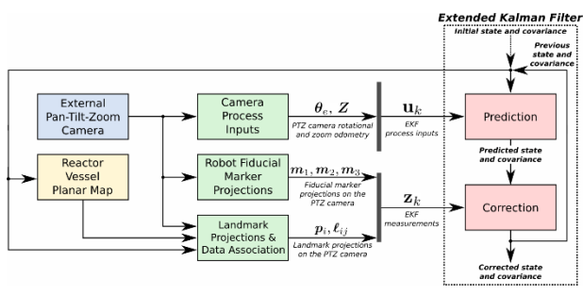

State Estimation and Localization

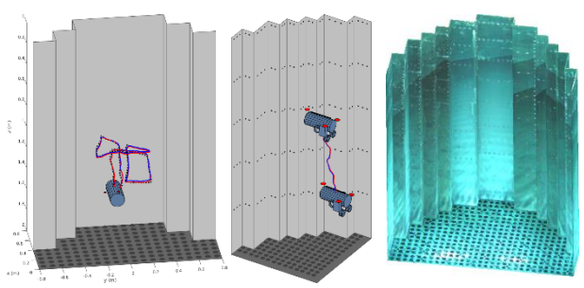

Results

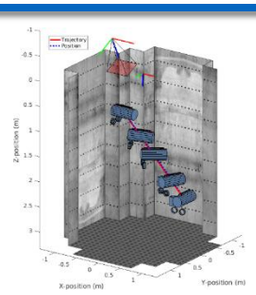

Conclusion and Future Work

Conclusion

1. We have **developed a state estimation framework for ROV localization** with a reactor lower core using a pan-tilt-zoom camera.
   - The framework leverages a **planar representation** of the reactor core.
   - The framework is shown to be successful for a variety of reactor mockups and settings.
   - The framework is **robust to environmental image degradation**, including speckling and color attenuation.
2. The system will be **deployed in real reactor inspection scenarios**.
3. The framework lays the foundation for impactful improvements to reactor inspections.
   - Greater utility and increasing efficiency through **automation via ROV navigation**.
   - Possible substantial process changes as a result of **new inspection opportunities** from dense reconstruction and visual review.

Inspection Automation via ROV Navigation

- Localization framework enables efficient, automated inspections through ROV navigation
  - Generation of time-efficient trajectories
  - Closed-loop feedback control of ROV position and heading through thruster inputs
- Preliminary navigation results achieved in simulation using a ROV dynamics model

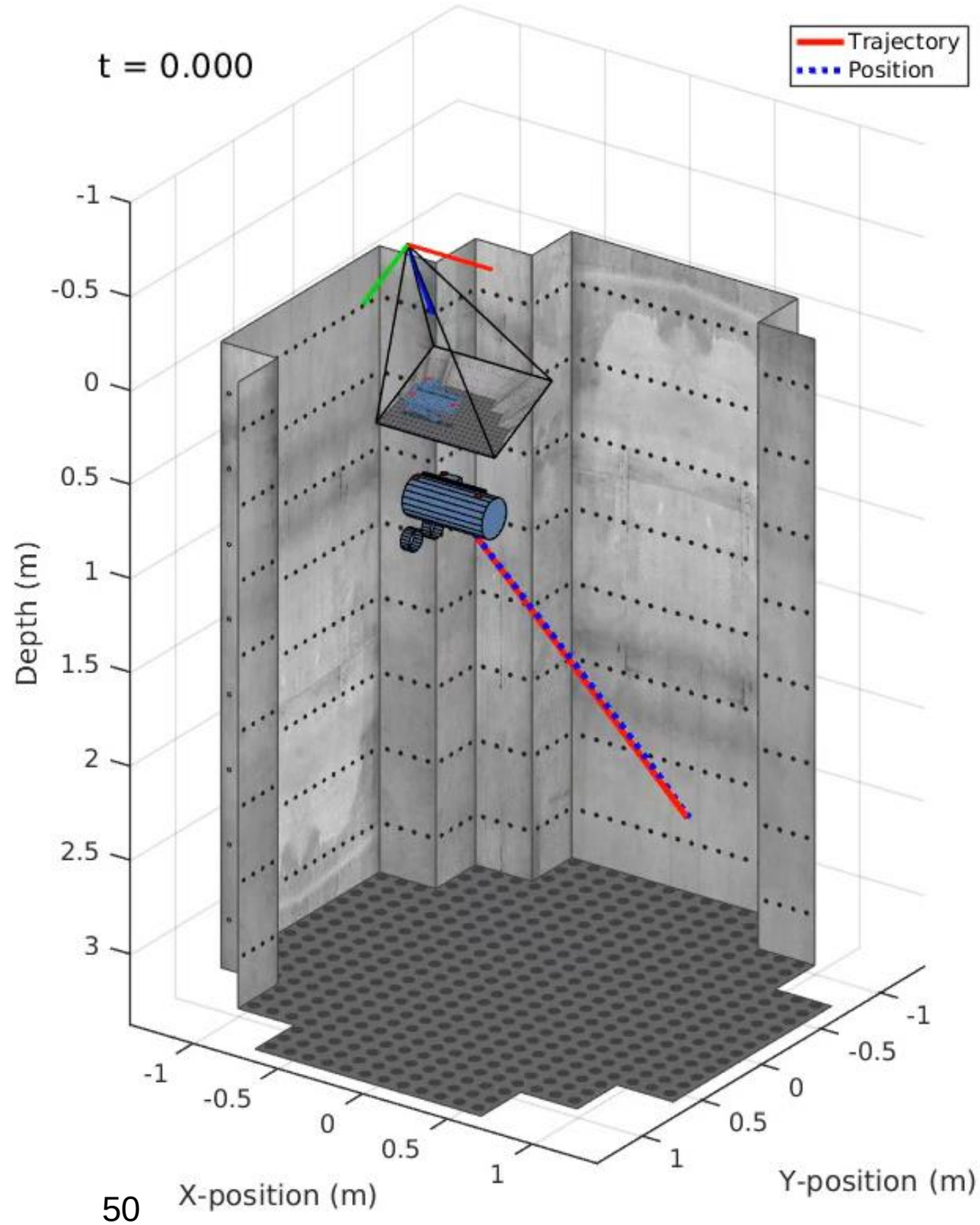

Acknowledgements

We gratefully acknowledge the research contributions of:

- Prof. Nathan Michael (CMU)
- Curtis Boirum (CMU)

We gratefully acknowledge the sponsorship of Westinghouse Electric Company, LLC.

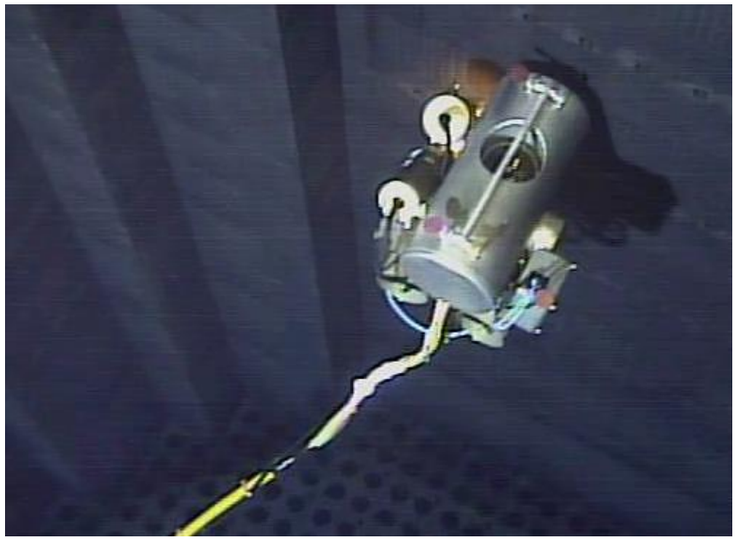

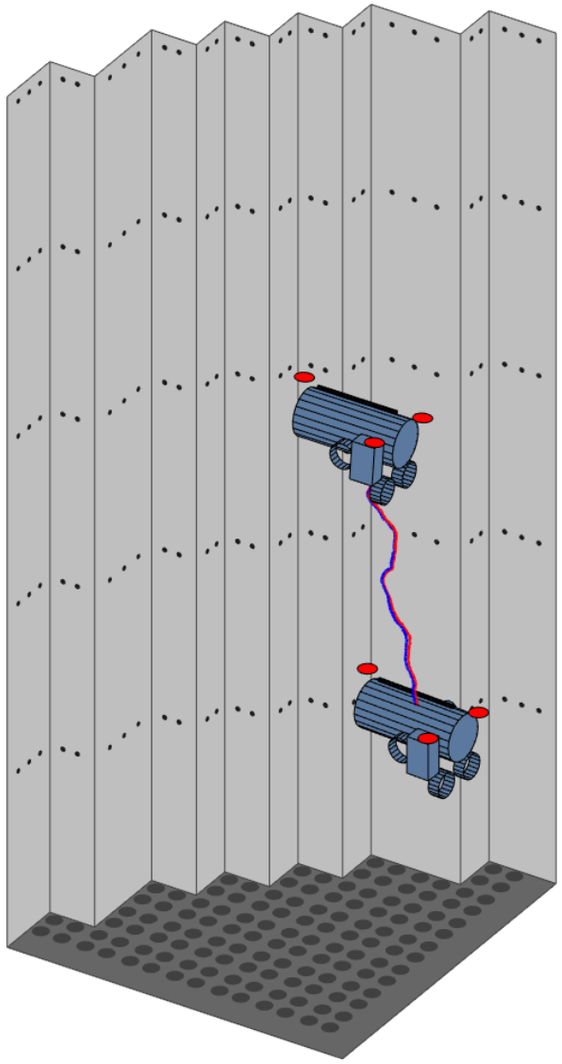

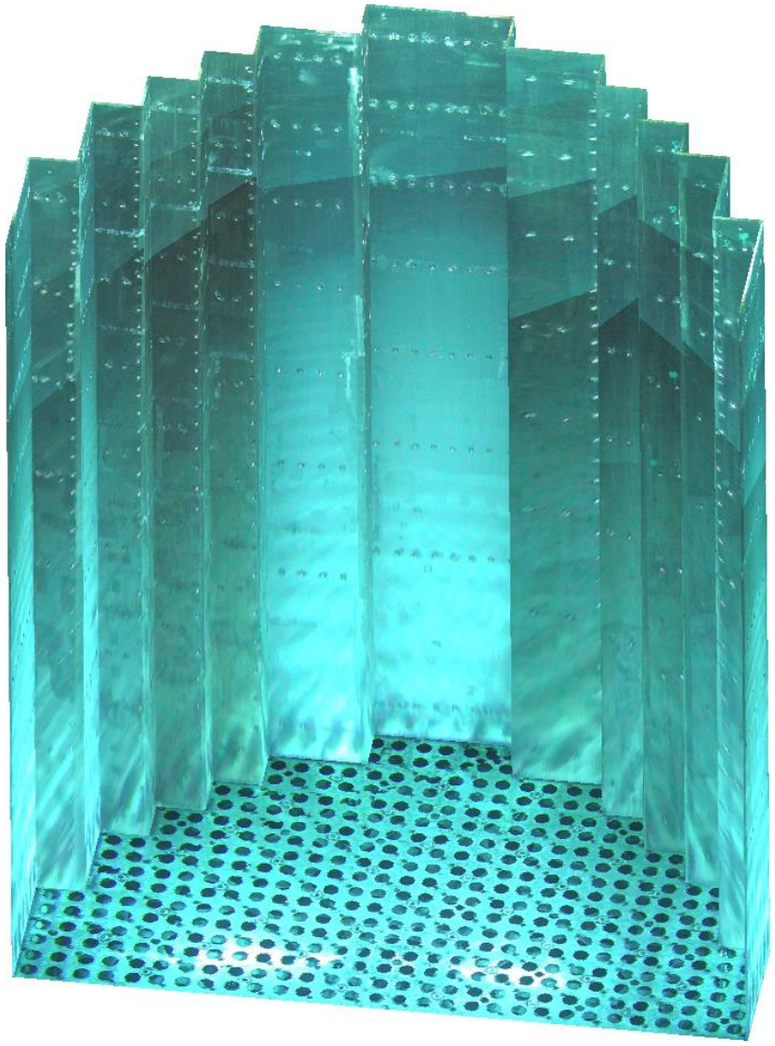

Questions and Discussion

Carnegie Mellon University
The Robotics Institute

Backup Slides

Carnegie Mellon University
The Robotics Institute

PTZ Camera Models: Orientation

- PTZ camera has two degrees of freedom: pan and tilt with respect to a base "scene frame"
- Pan axis fixed w.r.t. scene frame

$$\bar{\Theta} = [\,0,\ 1,\ 0\,]^{\mathrm{T}}$$

- Tilt axis fixed w.r.t. camera frame

$$\bar{\Phi} = [\,1,\ 0,\ 0\,]^{\mathrm{T}}$$

PTZ Video

- Camera orientation w.r.t world frame obtained from kinematic chain:[1]

$$R_e^w = R(R_s, \theta, \phi) = R_\phi R_\theta R_s$$

$$R_\theta = I_{3\times3} + (\sin\theta)\left[R_s\bar{\Theta}\right]_\times + (1-\cos\theta)\left[R_s\bar{\Theta}\right]_\times^2$$

$$R_\phi = I_{3\times3} + (\sin\phi)\left[R_\theta R_s\bar{\Phi}\right]_\times + (1-\cos\phi)\left[R_\theta R_s\bar{\Phi}\right]_\times^2$$

[1]Collins and Tsin (1999).

Zoom Variation for Underwater Optics

- Aspect ratio is constant for zoom variation in air

$$FOV_H(s) = 2\tan^{-1}\left(\frac{h}{2\mathfrak{f}s}\right)$$

$$FOV_V(s) = 2\tan^{-1}\left(\frac{v}{2\mathfrak{f}s}\right)$$

$$f_x(s) = \frac{c_x}{\tan\left(FOV_H(s)/2\right)} = \frac{2c_x\mathfrak{f}s}{h}$$

$$f_y(s) = \frac{c_y}{\tan\left(FOV_V(s)/2\right)} = \frac{2c_y\mathfrak{f}s}{v}$$

$$\tau = \frac{f_x(s)}{f_y(s)} = \frac{c_x v}{c_y h}$$

- Aspect ratio is *not* constant for a flat-plate housing underwater

$$f_{x,water}(s) = \frac{c_x}{\tan\left(FOV_{H,water}(s)/2\right)} = \frac{c_x}{h}\sqrt{(2\mathfrak{f}s)^2 n_w^2 + (n_w^2 - 1)h^2}$$

$$f_{y,water}(s) = \frac{c_y}{\tan\left(FOV_{V,water}(s)/2\right)} = \frac{c_y}{v}\sqrt{(2\mathfrak{f}s)^2 n_w^2 + (n_w^2 - 1)v^2}$$

$$\tau_{water}(s) = \frac{f_{x,water}(s)}{f_{y,water}(s)} = \frac{c_x v\sqrt{(2\mathfrak{f}s)^2 n_w^2 + (n_w^2 - 1)h^2}}{c_y h\sqrt{(2\mathfrak{f}s)^2 n_w^2 + (n_w^2 - 1)v^2}}$$

Speckling

- Speckling is stochastic chromatic image noise that is induced by radiation.
- We quantify a speckling model used for assessing framework robustness.

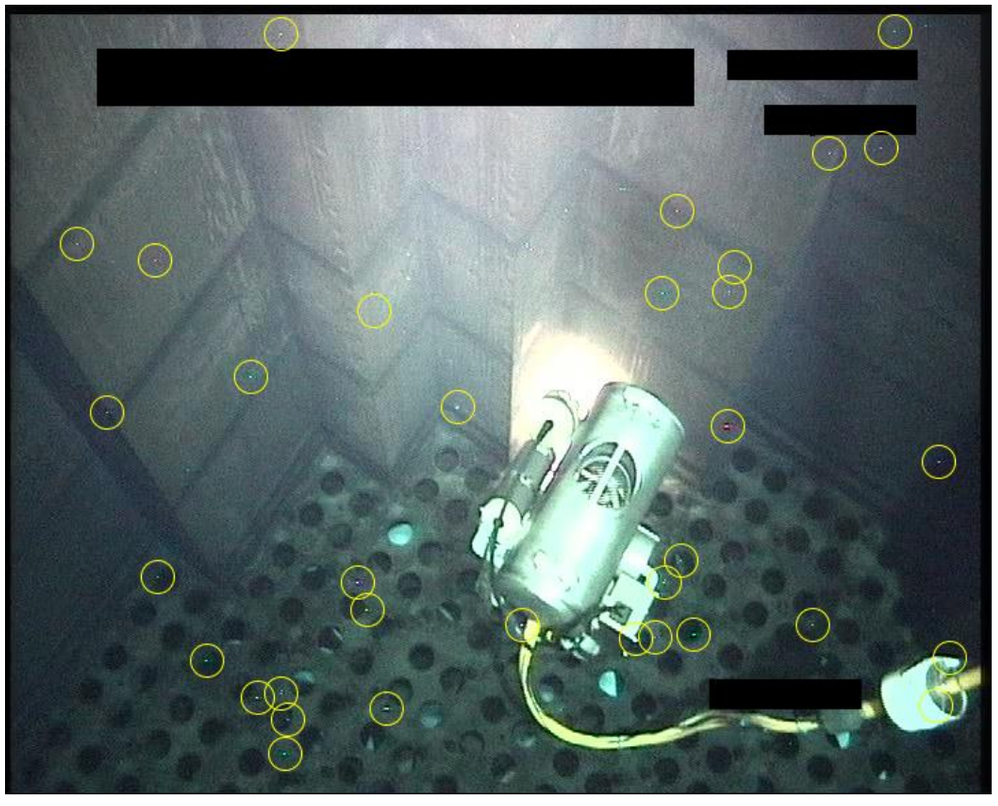

Speckling exhibited in a camera frame.

Parameter	Value
$n_{frame} \sim \mathcal{N}(\mu, \sigma^2)$	
μ	6.4655e−5
σ^2	3.0493e−10
$s_{size} \sim Cat(K_i, p_i)$	
$i = \{1, \ldots, 6\}, K_i = i$	
p_1	0.4034
p_2	0.4087
p_3	0.1021
p_4	0.0542
p_5	0.0200
p_6	0.0116

Speckling statistical model.

EKF Process Models: Covariance

- State covariance propagation

$$\bar{\Sigma}_k = G_k \, \Sigma_{k-1} \, {G_k}^{\mathrm{T}} + Q_k \qquad G = \frac{\partial g(\mathbf{u}, \mathbf{X})}{\partial \mathbf{X}} \quad V = \frac{\partial g(\mathbf{u}, \mathbf{X})}{\partial \mathbf{u}}$$

$$Q_k = W_k + V_k \, M_k \, {V_k}^{\mathrm{T}} \qquad G_k = G\big|_{\mathbf{u}_k, \, \boldsymbol{\mu}_{k-1}} \quad V_k = V\big|_{\mathbf{u}_k, \, \boldsymbol{\mu}_{k-1}}$$

- Process noise accounts for ROV random process and propagation of noise from input space to state space

$$M_k = \mathrm{diag}(\sigma_a^2 I_{3\times 3}, \, \sigma_z^2)$$

$$W_k = \mathrm{diag}(\sigma_r^2 I_{3\mathrm{x}3}, \, \sigma_q^2 I_{4\times 4}, \, 0_{N-7\times N-7})$$

EKF Measurement Models

- Two types of measurements:
  1. Camera-to-ROV
     - Marker projections
  2. Camera-to-World
     - Projection of vessel points
     - Projection of vessel lines

$$\mathbf{z} = [\, \mathbf{z}_b^{e\mathrm{T}}, \, \mathbf{z}_e^{w\mathrm{T}} \,]^{\mathrm{T}}$$

$$\hat{\mathbf{z}}_k = h(\mathbf{X}_k) + \mathcal{N}(0, R_k)$$

$$\Delta \mathbf{z}_k = \mathbf{z}_k - \hat{\mathbf{z}}_k$$

$$S_k = H_k \bar{\Sigma}_k {H_k}^{\mathrm{T}} + R_k$$

$$K_k = \bar{\Sigma}_k {H_k}^{\mathrm{T}} S_k^{-1}$$

$$\boldsymbol{\mu}_k = \bar{\boldsymbol{\mu}}_k + K_k \Delta \mathbf{z}_k$$

$$\Sigma_k = \bar{\Sigma} - K_k H_k \bar{\Sigma}_k$$

- All measurements in camera image space

$$H = \frac{\partial h(\mathbf{X})}{\partial \mathbf{X}}$$

$$H_k = H|_{\boldsymbol{\mu}_k}$$

EKF Measurement Models: Camera-to-ROV

- Marker projections provide observations for ROV pose
- Marker position uncertainty included in measurement uncertainty

$$\mathbf{z}_{m,k} = [\,\boldsymbol{m}_{1,k}{}^{\mathrm{T}},\ \boldsymbol{m}_{2,k}{}^{\mathrm{T}},\ \boldsymbol{m}_{3,k}{}^{\mathrm{T}}\,]^{\mathrm{T}}$$

$$h_m(\mathbf{X}_k) = [\,\hat{\boldsymbol{m}}_{1,k}{}^{\mathrm{T}},\ \hat{\boldsymbol{m}}_{2,k}{}^{\mathrm{T}},\ \hat{\boldsymbol{m}}_{3,k}{}^{\mathrm{T}}\,]^{\mathrm{T}}$$

$$R_{m,k} = \sigma_I^2 I_{6\times 6} + J_k \left(\sigma_M^2 I_{9\times 9}\right) J_k{}^{\mathrm{T}}$$

$$J_{ij} = \frac{\partial \mathbf{m}_i}{\partial \mathbf{M}_j^b}, \quad \forall i, j = \{1,\ 2,\ 3\} \quad J_k = J\big|_{\boldsymbol{\mu}_k}$$

EKF Measurement Models: Camera-to-World

- Point projections
  - Projection of floor (core plate) landmarks
  - Projection of wall (baffle plate) landmarks

- Line projections: $[\boldsymbol{p}_A{}^{\mathrm{T}}, \boldsymbol{p}_B{}^{\mathrm{T}}]^{\mathrm{T}} = [u_A, v_A, u_B, v_B]^{\mathrm{T}} \in \mathbb{R}^4$
  - Projection of Plücker lines between adjacent walls
  - Projection of Plücker lines between wall and floor
  - Projection of Plücker lines between wall and top rim

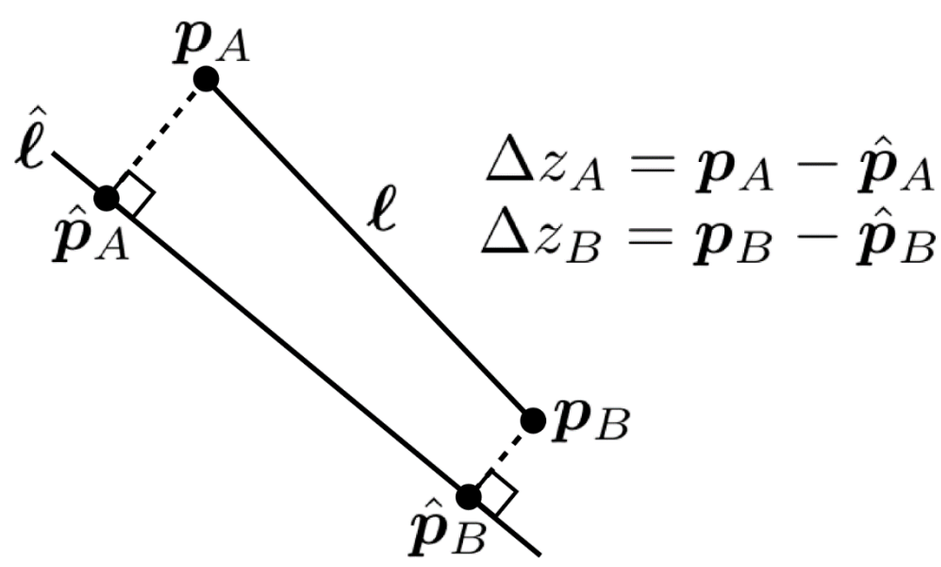

Error function between a predicted line and observed line segment.

EKF Measurement Models: Camera-to-World

- Measurement model for Plücker lines between walls

$$\hat{\mathbf{z}}_{wl,\,k,\,i} = h_{wl}(\mathbf{X}_k) + \mathcal{N}(0, R_{k,\,ln})$$

$$\mathbf{z}_{wl,\,k,\,i} = \begin{bmatrix} \boldsymbol{p}_{wl,\,A,\,k,\,i} \\ \\ \boldsymbol{p}_{wl,\,B,\,k,\,i} \end{bmatrix} \qquad h_{wl}(\mathbf{X}_k) = \begin{bmatrix} \hat{\boldsymbol{p}}_{wl,\,A,\,k,\,i} \\ \\ \hat{\boldsymbol{p}}_{wl,\,B,\,k,\,i} \end{bmatrix}$$

$$\hat{\boldsymbol{\ell}} \sim \hat{\mathcal{K}}\hat{\mathcal{D}}^e_w \hat{\boldsymbol{\mathcal{L}}}^w_{wl,\,i}$$

$$\hat{\boldsymbol{\mathcal{L}}}^w_{wl,\,i} \sim \hat{\boldsymbol{\pi}}_i \wedge \hat{\boldsymbol{\pi}}'_i$$

$$\hat{b} = -\frac{1}{\hat{\ell}_y}, \quad \hat{b}_{\perp,\,A} = v_A - m_\perp u_A, \quad \hat{b}_{\perp,\,B} = v_B - m_\perp u_B$$

$$\hat{m} = -\frac{\hat{\ell}_x}{\hat{\ell}_y}, \quad \hat{m}_\perp = -\frac{1}{\hat{m}}$$

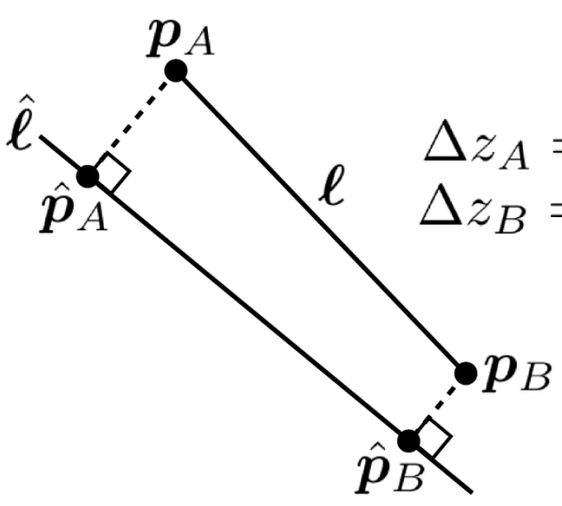

$$\Delta z_A = \boldsymbol{p}_A - \hat{\boldsymbol{p}}_A$$
$$\Delta z_B = \boldsymbol{p}_B - \hat{\boldsymbol{p}}_B$$

$$\hat{\boldsymbol{p}}_{wl,\,A,\,k,\,i} = \begin{bmatrix} \hat{u}_{wl,\,A,\,k,\,i} \\ \\ \hat{v}_{wl,\,A,\,k,\,i} \end{bmatrix} = \begin{bmatrix} \frac{\hat{b}_{\perp,\,A} - \hat{b}}{\hat{m} - \hat{m}_\perp} \\ \\ \hat{m}\,\hat{u}_{wl,\,A,\,k,\,i} + \hat{b} \end{bmatrix}$$

$$\hat{\boldsymbol{p}}_{wl,\,B,\,k,\,i} = \begin{bmatrix} \hat{u}_{wl,\,B,\,k,\,i} \\ \\ \hat{v}_{wl,\,B,\,k,\,i} \end{bmatrix} = \begin{bmatrix} \frac{\hat{b}_{\perp,\,B} - \hat{b}}{\hat{m} - \hat{m}_\perp} \\ \\ \hat{m}\,\hat{u}_{wl,\,B,\,k,\,i} + \hat{b} \end{bmatrix}$$

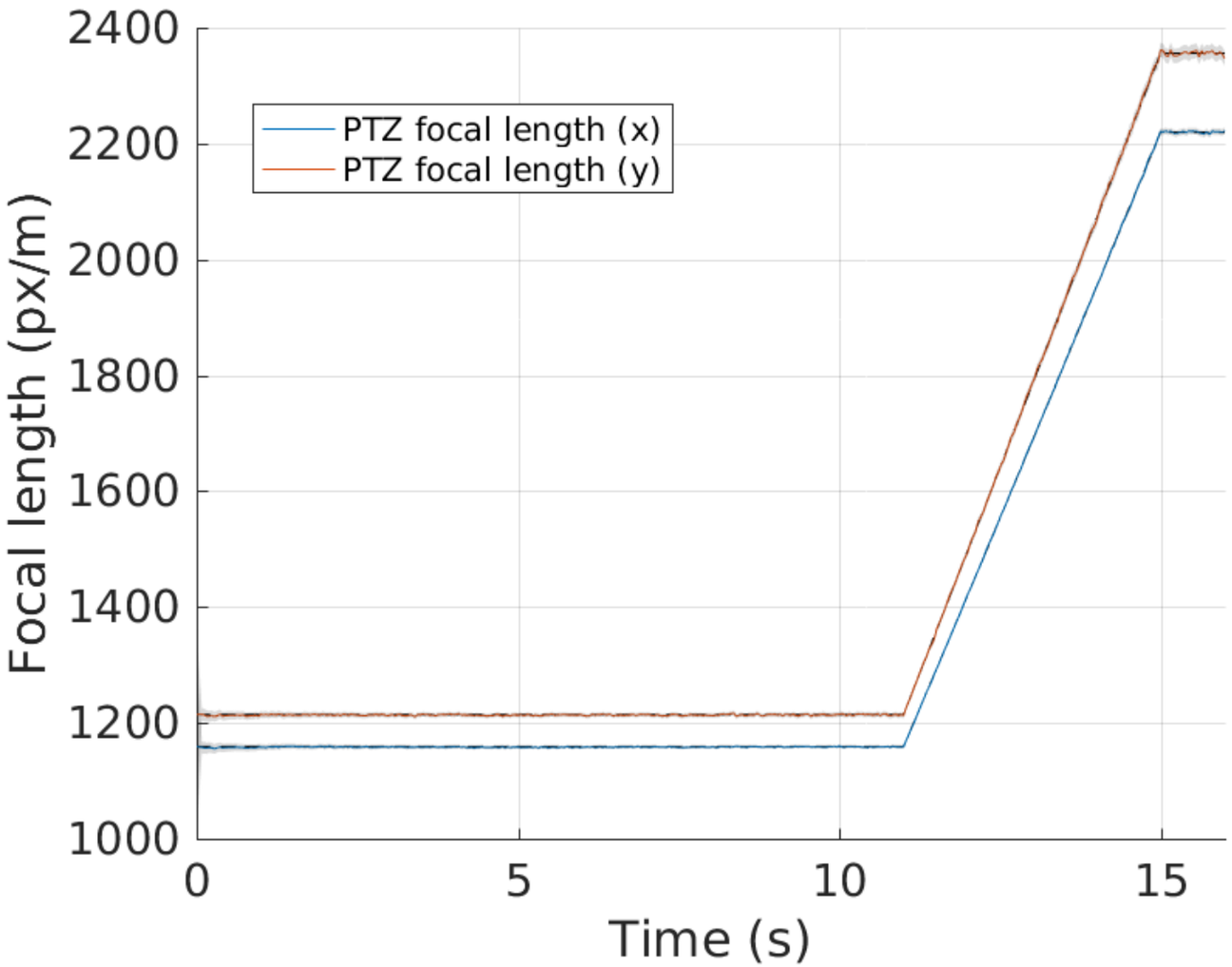
PTZ focal length (x)
PTZ focal length (y)
Focal length (px/m)
2400
2200
2000
1800
1600
1400
1200
1000
0
5
10
15
Time (s)

Online ROV Initialization